

PARAMETER IDENTIFICATION  
PARAMETER IDENTIFICATION  
IN A LAYERED AQUIFER SYSTEM  
IN A LAYERED AQUIFER SYSTEM

*Pamela G. Anderson*  
Pamela G. Anderson

A Thesis

Presented to

the Faculty of the Department of Civil and  
Environmental Engineering  
University of Houston

Committee Members:

*K.H. Wang*  
K.H. Wang, Associate Professor,

In Partial Fulfillment

of the Requirements for the Degree

Master of Science

in Civil Engineering

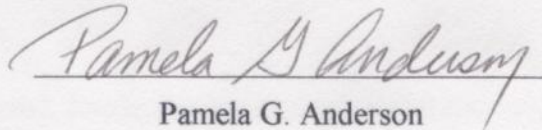
by

*Charles Dalton*  
Charles Dalton, Associate Dean  
Cullen College of Engineering

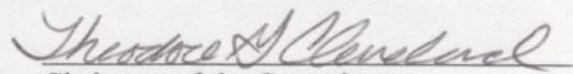
*Pamela G. Anderson*  
Pamela G. Anderson, Professor and Chairman,  
Department of Civil and Environmental Engineering

May 1997

PARAMETER IDENTIFICATION  
IN A LAYERED AQUIFER SYSTEM


  
Pamela G. Anderson

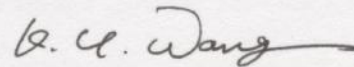
Approved:

  
Chairman of the Committee

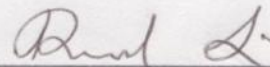
Theodore G. Cleveland, Associate Professor,  
Civil and Environmental Engineering

Committee Members:

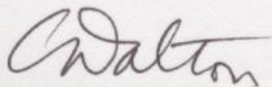




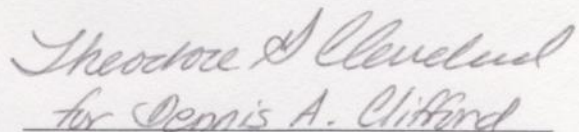
K.H. Wang, Associate Professor,  
Civil and Environmental Engineering



Richard C. Liu, Associate Professor,  
Electrical and Computer Engineering



Charles Dalton, Associate Dean  
Cullen College of Engineering



Dennis Clifford, Professor and Chairman,  
Civil and Environmental Engineering



## Acknowledgments

I gratefully acknowledge my research advisor, Dr. Theodore Cleveland, for giving me the opportunity to perform this research and for his support, guidance, and insight throughout the research.

I thank my husband, David, for his support, understanding, and suggestions during my studies at the University of Houston. I would also like to thank my parents, the late Hugh Gebhardt and Martha Gebhardt for their lifelong encouragement and support. I would also like to thank the rest of my family for their support and understanding.

I thank Dr. K.H. Wang, Dr. Richard C. Liu, and Dr. Michael W. O'Neill for their suggestions and recommendations.

**This Thesis is dedicated to**

**Hugh E. Gebhardt**

I express my appreciation to my fellow graduate student, Lu-chia Chuang, for his assistance and computer expertise.

I thank Tracy Nishikawa and Randy Hanson of the USGS for the field data used in the research and their interest in my work.

And, finally, I acknowledge the Department of Civil and Environmental Engineering and the Office of the Dean for their financial support during my research.

## Acknowledgments

I gratefully acknowledge my research advisor, Dr. Theodore Cleveland, for giving me the opportunity to perform this research and for his support, guidance, and insight throughout the research.

I thank my husband, David, for his support, understanding, and suggestions during my studies at the University of Houston. I would also like to thank my parents, the late Hugh Gebhardt and Martha Gebhardt for their lifelong encouragement and support. I would also like to thank the rest of my family for their support and understanding.

I thank Dr. K.H. Wang, Dr. Richard C. Liu, and Dr. Michael W. O'Neill for their suggestions and recommendations.

I express my appreciation to my fellow graduate student, Lu-chia Chuang, for his assistance and computer expertise.

I thank Tracy Nishikawa and Randy Hanson of the USGS for the field data used in the research and their interest in my work.

And, finally, I acknowledge the Department of Civil and Environmental Engineering and the Office of the Dean for their financial support during my research.

by

Paula G. Anderson

May 1997



**PARAMETER IDENTIFICATION  
IN A LAYERED AQUIFER SYSTEM**

**An Abstract**

**of a**

**Thesis**

**Presented to**

**the Faculty of the Department of Civil**

**and Environmental Engineering**

**University of Houston**

**In Partial Fulfillment**

**of the Requirements for the Degree**

**Master of Science**

**in Civil Engineering**

**by**

**Pamela G. Anderson**

**May 1997**

## Abstract

Inverse analysis of aquifer parameters has been typically performed using trial-and-error methods. The complexity of these analyses increases with the number of layers in the system. In addition, flowmeter data has been shown to be an excellent source of layer information, but cannot be used to infer storage properties. The purpose of this research was to assemble a package of computer programs to evaluate characteristic parameters for a multilayer aquifer system using data obtained from pumping and flowmeter tests and from observations in nearby wells. The LAPIS package consists of a groundwater modeling program and an optimizing program. Testing of the package showed good agreement with analytical solutions. Analysis of actual field data showed the use of flowmeter data could provide valuable information in the parameter analysis of a multilayer system. We were also able to modify the parameters in a logical, systematic approach, thereby automating and improving the analysis.

Difficulties in Inverse Analyses .....	10
The Use of Parameter Identification Methods .....	12
Analysis of Flowmeter Data .....	12
Analysis of Hydraulic Conductivity Using Flowmeter Data .....	16
Chapter 4 - Groundwater Model Design .....	19
General .....	19
Hopscotch Algorithm .....	19
Model Development .....	22
Testing and Results .....	30



## Table of Contents

	<u>Page</u>
Acknowledgments .....	v
Abstract.....	vii
List of Figures .....	x
List of Tables.....	xi
Notation .....	xii
Chapter 1 - Introduction .....	1
Chapter 2 - Purpose.....	4
Analysis of Problem.....	4
Objective of Research.....	6
Chapter 3 - Literature Review.....	8
Flowmeters.....	8
Difficulties in Inverse Analyses .....	10
The Use of Parameter Identification Methods .....	12
Analysis of Flowmeter Data.....	12
Analysis of Hydraulic Conductivity Using Flowmeter Data .....	16
Chapter 4 - Groundwater Model Design .....	19
General.....	19
Hopscotch Algorithm .....	19
Model Development .....	22
Testing and Results .....	30

Chapter 5 - General Approach .....	32
General.....	32
Groundwater Modeling Program .....	32
Optimizer Program.....	36
Processor Program.....	38
Chapter 6 - Package Testing .....	41
Methodology.....	41
Testing using the Theis Solution .....	41
Testing using the Hantush Solution.....	44
Findings.....	48
Chapter 7 - Data Analysis .....	49
General.....	49
Description of Field Data.....	49
Model Configuration .....	51
Testing.....	58
Results .....	60
Chapter 8 - Conclusions and Recommendations .....	67
References .....	69
Bibliography .....	72
Appendix.....	74
GCOMP Source Code.....	75
Sample Input File .....	84



## List of Figures

Figure 3-1: Typical Flowmeter Data Plot .....	9
Figure 4-1: Hopscotch Model Flowchart.....	29
Figure 4-2: Drawdown vs. Time - Hopscotch Analysis.....	31
Figure 5-1: MODFLOW Conductance Diagram.....	35
Figure 5-2: GCOMP Flowchart.....	39
Figure 6-1: Aquifer Configuration - Theis Solution .....	42
Figure 6-2: Aquifer Configuration - Hantush Solution.....	44
Figure 7-1: Site Geology.....	50
Figure 7-2: Flowmeter Data .....	52
Figure 7-3: Drawdown vs. Time - Layer 3 .....	63
Figure 7-4: Drawdown vs. Time - Layer 5 .....	64

## List of Tables

Table 6-1: Summary of Results of Hantush Analyses.....	46
Table 7-1: Layer Information.....	51
Table 7-2: Transmissivity Calculations.....	55
Table 7-3: Summary of Test Cases.....	59
Table 7-4: Results of Case 1 Analysis.....	62
Table 7-5: Summary of Results of Analyses- Layer 3 .....	65
Table 7-6: Summary of Results of Analyses- Layer 5 .....	66

$d$	- Drawdown
$g$	- Acceleration due to Gravity
$h$	- Head
$K$	- Hydraulic Conductivity
$K(z)$	- Hydraulic Conductivity that Varies with Depth
$K_i$	- Horizontal Hydraulic Conductivity of Layer $i$
$K_x$	- Horizontal Hydraulic Conductivity
$K_v$	- Vertical Hydraulic Conductivity between Layers
$\bar{K}$	- Average or Bulk Hydraulic Conductivity of a Layered Aquifer
$Q$	- Discharge in a Borehole or Screened Well
$Q(z)$	- Discharge in a Borehole or Screened Well at a Particular Depth
$QP$	- Total Discharge Produced by Pump
$q$	- Discharge or Rate of Groundwater Flow in Layer $i$
$q_n$	- Flow into a Node
$q_{out}$	- Flow out of a Node



## Notation

- $r$  - Distance from the Pumping Well to the Observation Well
- $r_w$  - Radius to the Well
- A - Cross-Sectional Area of Flow
- B - Aquifer Thickness or Total Thickness of a Layered Aquifer
- C - Hydraulic Conductance
- $C_r$  - Conductance in a Radial Direction
- CC - Conductance Flow through a Column Face
- CR - Conductance Flow through a Row Face
- CV - Conductance Flow through a Layer Face
- $T$  - Transmissivity
- d - Drawdown
- g - Acceleration due to Gravity
- h - Head
- K - Hydraulic Conductivity
- $K(z)$  - Hydraulic Conductivity that Varies with Depth
- $K_i$  - Horizontal Hydraulic Conductivity of Layer i
- $K_r$  - Horizontal Hydraulic Conductivity
- $K_v$  - Vertical Hydraulic Conductivity between Layers
- $\bar{K}$  - Average or Bulk Hydraulic Conductivity of a Layered Aquifer
- Q - Discharge in a Borehole or Screened Well
- $Q(z)$  - Discharge in a Borehole or Screened Well at a Particular Depth
- QP - Total Discharge Produced by Pump
- q - Discharge or Rate of Groundwater Flow in Layer i
- $q_{in}$  - Flow into a Node
- $q_{out}$  - Flow out of a Node

- $r$  - Distance from the Pumping Well to the Observation Well
- $r_i$  - Radius to the  $i$ -th Node
- $r_w$  - Effective Well Radius
- $S$  - Storativity
- $S_i$  - Storativity for Layer  $i$
- $S_s$  - Specific Storage Coefficient, also  $S_s$
- $S_y$  - Specific Yield
- $t$  - Elapsed Time in Pumping Test
- $T$  - Transmissivity
- $w$  - Volumetric Source/Sink Rate
- $z$  - Depth
- $\alpha$  - Radius Multiplication Factor (Chapter 4)
- $\alpha$  - Compressibility Coefficient of the Porous Medium (Chapter 7)
- $\beta_l$  - Compressibility of the Liquid
- $\beta_s$  - Compressibility of the Solid
- $\gamma$  - Unit Weight or  $\rho g$
- $\Delta h$  - Change in Head or Drawdown
- $\Delta Q_i$  - Discharge in a Borehole or Screened Well for Layer  $i$  in an Aquifer
- $\Delta z_i$  - Thickness of Layer  $i$
- $\Delta x$  - Width of Row in MODFLOW Grid
- $\Delta y$  - Width of Column in MODFLOW Grid
- $\rho$  - Mass per Unit Volume or Density
- $\omega$  - Porosity



## Chapter 1 - Introduction

Numerous groundwater models and computer programs are currently being used. Additional input consists of a description of the aquifer configuration and pumping rate. These models generally require aquifer characteristics and a pumping rate as input to compute the drawdown or head associated with that data. In practice however (i.e., pumping tests or flowmeter tests), the pumping rate and drawdown are known, while the aquifer characteristics are not. Aquifer parameters are typically evaluated using a trial-and-error approach with multiple runs of a groundwater modeling program. The procedure is called inverse analysis.

The complexity of the inverse analysis increases with the number of layers. Prior work has shown that the inverse analysis of a multilayer system is extremely difficult when the only available data are observed drawdowns and a pumping or injection rate. Flowmeter data has been shown to be an excellent source of layer information, but cannot provide data to infer storage properties. The combination of information can, in principle, be used to improve the parameter analysis of a multilayer system.

The LAPIS package developed in this research combines an optimizer called GRG2, developed by Lasdon and Waren (1989), with a modular, groundwater flow model (MODFLOW) developed by McDonald and Harbaugh (1988). The GRG2 program uses the Generalized Reduced Gradient Method to solve nonlinear problems. In this research, the LAPIS package minimizes a merit equation based on a series of variables, the aquifer parameters. The MODFLOW program computes the drawdown associated with each set of trial values of the parameters.

Aquifer parameters used in the package consist of transmissivity, storativity, and vertical hydraulic conductivity of each layer in the aquifer or aquifers under consideration. Additional input consists of a description of the aquifer configuration and pumping rate. Aquifer configuration includes the size of the aquifer, number of layers, and well locations.

The use of an optimizer provides for a systematic approach to modifying the characteristic parameters, as opposed to the random approach used with trial-and-error analysis. The LAPIS package also automates the analysis, performing numerous parameter adjustments and checking the effect on the model drawdowns. This automated procedure allows the user to step away from the analysis and perform other work.

The package was tested against known solutions using the Theis and Hantush analytical solutions to verify its ability to "find" the correct answer. The package was then used on actual observation data provided by the U.S. Geological Survey (USGS). The evaluation of this same set of aquifer data was discussed in Hanson and Nishikawa (1996). They developed aquifer parameters using a trial-and-error approach.

The testing of the package showed good agreement with analytical solutions, validating the approach for this analysis. The analysis of actual field data showed that the use of flowmeter data provided useful additional information. This research also showed that the parameters could be modified in a logical, systematic method, thereby allowing the analysis of a multilayer system to be automated.

Initial research included the development of a groundwater model using a mixed explicit-implicit scheme. A finite-difference scheme, called Hopscotch (Lapidus and Pinder, 1982), was used. According to Lapidus and Pinder (1982), the Hopscotch



algorithm has the calculation ease of an explicit solution with the overall stability of an implicit solution. The research determined that although the algorithm was stable over the long time frame, large time steps produced large oscillations in the early phases of the analysis before finally converging on a solution. These large oscillations were unacceptable, since the early time steps are critical for the evaluation of storativity. The promise of the Hopscotch method was complete spreadsheet analysis. Unfortunately, the large oscillations at early time steps forced abandonment of this approach for the implicit capabilities in MODFLOW, a commonly used groundwater-flow modeling tool.

## Chapter 2 - Purpose

### Analysis of Problem

There are a number of models commonly used for groundwater flow analysis. These include analytical methods, such as the Theis solution or the Hantush method, and numerical models. Examples of numerical models routinely used are MODFLOW, developed by the USGS (McDonald and Harbaugh, 1988), and AX (Rutledge, 1991). Although the models differ in their actual input/output requirements, they generally all require the same fundamental parameters for input and produce heads or drawdowns as output. The aquifer parameters required for each layer include horizontal and vertical hydraulic conductivity, layer thickness, and storativity. Hydraulic conductivity describes the rate at which water can move through a permeable medium. Storativity, or storage coefficient, is the volume of water released from or taken into storage per unit surface area of the aquifer per unit change in head. Transmissivity is often used in the input instead of hydraulic conductivity. Transmissivity is the horizontal hydraulic conductivity of the aquifer or layer times its thickness.

The input also includes the aquifer configuration and the pumping or injection rate on the aquifer. The models vary in their analysis algorithm and the type of additional input required or additional output data produced.

However, conditions are quite different in the field. A stress event, such as the pumping or injection, is induced on the aquifer, and heads are measured at some distance or distances from the source well. This is commonly known as a stress test. Heads, and



therefore drawdowns, are the data produced from these field tests. The aquifer parameters cannot be directly determined in the field by pumping or injecting the aquifer.

The aquifer parameters can be evaluated from laboratory tests on samples of the aquifer materials or by iterative analyses of the data collected during a stress test. However, Capuano and Jan (1996), Daniel (1984), and Elsbury, et al. (1990) showed that samples tested in the laboratory had permeabilities (or hydraulic conductivities) that were anywhere from 25 to 2000 times smaller than those measured in the field. Therefore, iterative or trial-and-error analysis of field data is the most commonly used method for evaluating aquifer parameters. Laboratory testing can provide a starting point in an analysis, but should not be used for the final answer or for evaluating engineering designs.

However, trial-and-error analysis is not without its problems. In this type of analysis, the user must go through the following steps:

- Set up the model.
- Make an initial estimate of the parameters.
- Develop the input files and run the program.
- Review the results and develop new parameters.
- Revise the input files and run the program again until the model and observed drawdowns are within the selected tolerance.

As suggested above, this type of analysis is very time intensive. Secondly, there is no systematic method of modifying the parameters. In addition, the effort involved in the analysis of the aquifer parameters is a function of the number of layers. The more layers there are in the system, the more complex the analysis can become. There are three

parameters for each layer, except for the lowest layer. Therefore, separate trial runs must be made to evaluate the effect of each parameter. Then, the effect of combinations of the parameters must be addressed.

In addition, the analysis of multilayer aquifer systems using only pumping rates and drawdown data is extremely difficult. These data do not provide any indication as to the contribution of each layer to the overall flow. In instances where flowmeter tests have been performed in conjunction with pumping tests, the flowmeter data can be used to delineate aquifer layers with different characteristic properties. A flowmeter is a piece of equipment placed in a well that measures the flow rate. Flowmeter data can also be used to provide a better first estimate of some of the aquifer parameters. Flowmeter data is relatively convenient, and, after the initial equipment investment, inexpensive to collect.

A review of these difficulties provided the impetus to investigate combining the data to improve the success of automated analysis.

#### Objective of Research

Objective. The objective of this research was to develop a groundwater modeling package to evaluate characteristic parameters for a multilayer aquifer system using data obtained from pumping and flowmeter tests at a single well with observations at one or more, nearby nonpumping wells. This objective was accomplished by combining an axisymmetric groundwater flow model with an optimizer program to evaluate methodically the different aquifer parameters.

Specific Goals. I had three specific goals in meeting the objective. First, I wanted to demonstrate the value and validity of using flowmeter data in the analysis of a



multilayer system. Flowmeter data provide additional information about the aquifer characteristics that is critical in the analysis of multilayer systems.

#### Flowmeters

Secondly, I wanted to automate the iterative inverse analysis of aquifer parameters.

This would relieve the user of the tedious trial-and-error analysis commonly used.

Lastly, I wanted to replace the random nature of parameter modification used in trial-and-error analyses with a more logical, systematic approach. This systematic modification also made the automation component possible.

Flowmeters have been used in the petroleum industry for decades and the technology is easily transferred to groundwater application. The use of flowmeter technology allows one to get away from the common practice of averaging hydraulic conductivity in the vertical direction. Typical flowmeters used for measuring discharge in a borehole or screened well include heat-pulse or impeller technology (Moiz et al. 1989). Moiz et al. also states that most low-flow sensitive meters are based on heat-pulse or tracer release technology, but these are not usually commercially available. The impeller or spinner-type flowmeter is most commonly used in aquifer testing. This type of flowmeter includes an impeller mounted on a long rod with equipment capable of measuring the spin rate of the impeller. With respect to this research, any mention of flowmeters refers to the impeller type technology.

In a flowmeter test, the flowmeter is lowered to the bottom of the well. Then, a small pump is placed in the well or borehole and operated at a constant flow rate. Once a constant flow rate is obtained, the flowmeter impeller is started. The spin rate of the impeller is measured and recorded. This spin rate, or revolutions per time unit, is converted to flow velocity through calibration testing with known flow rates. After the spin rate is measured at the bottom of the well, the flowmeter is raised a depth increment (usually a few inches or feet), and another reading is taken. This process is repeated until the flowmeter reaches the top of the screened interval. Above the screened portion of the well, the flowmeter reading should roughly equal the steady flow rate of the pump,  $Q_p$ .

## Chapter 3 - Literature Review

### Flowmeters

Flowmeters have been used in the petroleum industry for decades, and the technology is easily transferred to groundwater application. The use of flowmeter technology allows one to get away from the common practice of averaging hydraulic conductivity in the vertical direction. Typical flowmeters used for measuring discharge in a borehole or screened well include heat-pulse or impeller technology (Molz et al. 1989). Molz et al. also states that most low-flow sensitive meters are based on heat-pulse or tracer release technology, but these are not usually commercially available. The impeller or spinner-type flowmeter is most commonly used in aquifer testing. This type of flowmeter includes an impeller mounted on a long rod with equipment capable of measuring the spin rate of the impeller. With respect to this research, any mention of flowmeters refers to the impeller type technology.

In a flowmeter test, the flowmeter is lowered to the bottom of the well. Then, a small pump is placed in the well or borehole and operated at a constant flow rate. Once a constant flow rate is obtained, the flowmeter impeller is started. The spin rate of the impeller is measured and recorded. This spin rate, or revolutions per time unit, is converted to flow velocity through calibration testing with known flow rates. After the spin rate is measured at the bottom of the well, the flowmeter is raised a depth increment (usually a few inches or feet), and another reading is taken. This process is repeated until the flowmeter reaches the top of the screened interval. Above the screened portion of the well, the flowmeter reading should roughly equal the steady flow rate of the pump,  $Q_P$ .



This procedure may be repeated in the same well to verify the flow rates. As illustrated in Fig. 3-1, the result is a series of data points giving vertical discharge or flow,  $Q$ , as a function of depth,  $z$ .

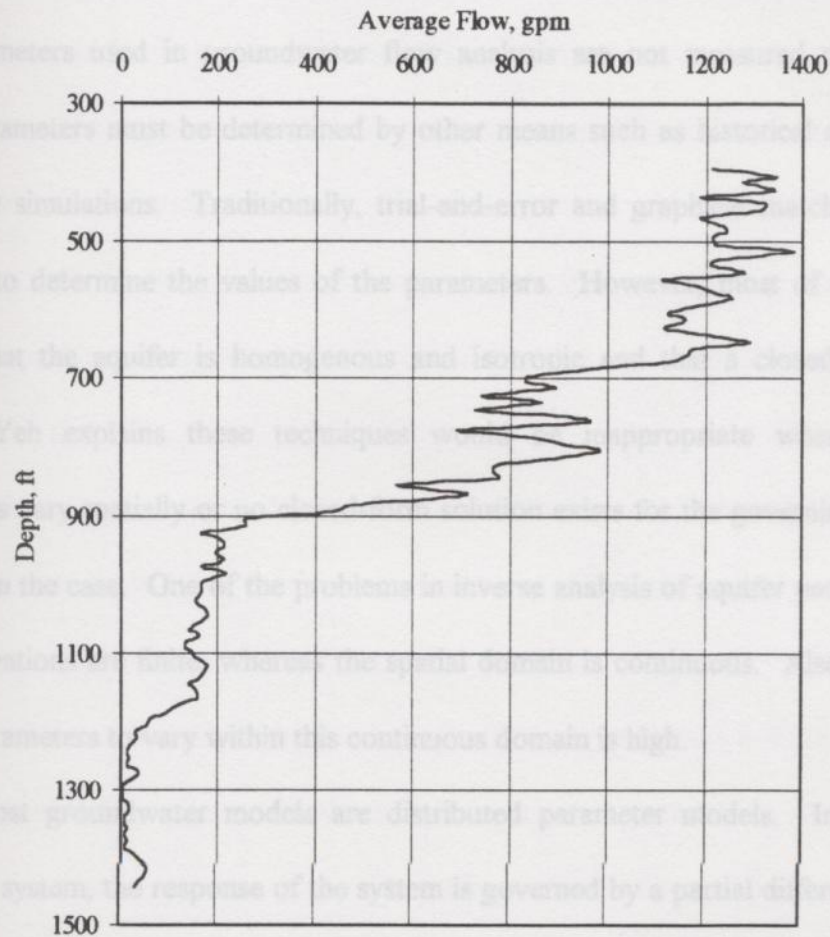


**Figure 3-1: Typical Flowmeter Data Plot**

The flow at any depth,  $Q(z)$ , is the total of all flow into the well below that point. The data is analyzed by looking for changes in average slopes. A change in average slope indicates a change in hydraulic conditions. Therefore, these changes in average slope can be used to discern layers with different hydraulic properties.

### Difficulties in Inverse Analyses

Part of the lack of use of inverse analysis methods is due to the inherent problems associated with that type of analyses, which can complicate the analysis. Yeh (1986) discussed problems associated with inverse analysis of groundwater hydrology parameters. The parameters used in groundwater flow analysis are not measured directly in situ. These parameters must be determined by other means such as historical observations or laboratory simulations. Traditionally, trial-and-error and graphical matching techniques are used to determine the values of the parameters. However, most of these solutions assume that the aquifer is homogenous and isotropic and that a closed-form solution exists. Yeh explains these techniques would be inappropriate where the aquifer parameters vary spatially or no closed-form solution exists for the governing equation, as is the often the case. One of the problems in inverse analysis of aquifer parameters is that the observations are finite, whereas the spatial domain is continuous. Also, the potential for the parameters to vary within this continuous domain is high.

Most groundwater models are distributed parameter models. In a distributed parameter system, the response of the system is governed by a partial differential equation and the parameters used in the equation are spatially dependent. Parameterization reduces the number of parameters from the infinite-dimension to the finite-dimension form.

Parameter identification methods have been classified as being one of two types, either the direct approach or the indirect approach (Yeh, 1986). The direct approach can be used if head variations and derivatives are known over the entire flow region and if the measurement and model errors are negligible. In practice, this is rarely the case.



Observation wells are sparsely distributed across the region, and only a limited amount of data from each well is available. To solve the inverse problem in this case, missing data or observations are estimated by interpolation. This interpolation introduces an error term into the governing equation or an equation error. In the direct approach, this equation error is minimized by the proper selection of parameter values.

The indirect approach is also called the output error criterion. In these methods, a "norm" of the difference between the observed and calculated heads at specific observation points is minimized. Advantages to this approach are that the formulation of the inverse problem is simplified and the formulation does not require the differentiation of the measured data (Yeh, 1986).

Yeh divided the types of errors associated with inverse problem into two groups:

- (1) system modeling error, represented by a performance criterion, and
- (2) the error associated with parameter uncertainty.

Yeh states that an increase in the number of unknown parameters will generally improve the system modeling error. However, this increase in parameters also increases the parameter uncertainty and vice versa. The optimum level of parameterization depends on the quantity and quality of the observation data.

In addition, the inverse problem is always characterized by nonuniqueness and instability of the identified parameters. The instability of the inverse solution occurs since small errors in heads will cause serious errors in the identified parameters. If the problem is nonunique, then the computed value of the parameter is related to the initial estimate, and may or may not be close to the "true" values of the parameters. In the case of

distributed parameters where only point measurements are available, the inverse problem is always nonunique. Point measurements refer to the case where measurements are made only at a limited number of locations.

#### The Use of Parameter Identification Methods

The interest in parameter identification methods was demonstrated by the convening of a special session at the Spring 1995 American Geophysical Union (AGU) meeting to discuss parameter identification and sensitivity analysis in groundwater flow and transport. An article reporting the discussion at the session stated that although methods for automated parameter identification were first developed at the same time as numerical groundwater models, these methods are rarely used (Hill and Zheng, 1995).

Participants at the meeting discussed current field and laboratory parameter identification studies. It was stated at the session that "the lack of physical complexity" in the models and "the confusing input requirements of the programs" were a factor in the continued use of trial-and-error methods. Another factor is the nonlinearity of the solution of the groundwater equations with respect to many estimated parameters. The participants discussed ten current studies that applied parameter identification. All of the programs discussed used a least-squares objective function, and the optimal parameters were generally computed by nonlinear regression methods.

#### Analysis of Flowmeter Data

Molz et al. (1989) discusses using an impeller-type flowmeter in groundwater applications. The paper presents a method, the  $K_i / \bar{K}$  profile method, for solving for the horizontal hydraulic conductivity of each layer using data from flowmeter testing. In this



study, the values computed using this proposed method were compared to those computed from tracer and multi-slug tests in the same aquifer.

In development of their method, Molz et al. started with the Cooper-Jacob formula for horizontal flow to a well from layer  $i$  of thickness  $\Delta z_i$ . The Cooper-Jacob formula states

$$\Delta h_i(r_w, t) = \frac{\Delta Q_i}{2\pi K_i \Delta z_i} \ln \left[ \frac{1.5 \left( \frac{K_i (\Delta z_i) t}{S_i} \right)^{1/2}}{r_w} \right], \quad (3-1)$$

where  $\Delta h_i$  - change in head or drawdown in layer  $i$ ,

$\Delta Q_i$  - flow from layer  $i$ ,

$K_i$  - horizontal hydraulic conductivity of layer  $i$ ,

$r_w$  - effective well radius,

$t$  - time since pumping began, and

$S_i$  - storativity of layer  $i$ .

Solving Eq. (3-1) for the  $K_i$  outside the log term yields

$$K_i = \frac{\Delta Q_i}{2\pi \Delta h_i \Delta z_i} \ln \left[ \frac{1.5 \left( \frac{K_i (\Delta z_i) t}{S_i} \right)^{1/2}}{r_w} \right] \quad (3-2)$$

which, traditionally, is solved iteratively for  $K_i$ . Molz et al. assumed that flow at the well becomes horizontal. Under this conditions, the radial gradients along the well bore are constant and uniform, and the flow into the well from a given layer is proportional to the transmissivity of the layer. Based on this information, Molz et al. were able to reduce

Eq. (3-2) to

$$\frac{K_i}{\bar{K}} = \frac{\Delta Q_i / \Delta z_i}{QP / B}, \quad (3-3)$$

where  $\bar{K}$  - the bulk horizontal hydraulic conductivity for the aquifer,

QP - total discharge for the well, and

B - the aquifer thickness.

Once  $\Delta Q_i$  is estimated from the flowmeter data plot, Eq. (3-3) is computed for each layer.

The value of  $\bar{K}$  is usually determined from a large scale test such as a fully penetrating pumping test. Then, each  $K_i / \bar{K}$  value is multiplied by  $\bar{K}$  producing a  $K_i$  for each layer.

Equation (3-3) assumes that  $\Delta Q_i$  and QP are constant with time (steady-state condition), and that flow is horizontal to the well. Steady state usually occurs when

$$r^2 S / 4Tt < 0.001, \quad (3-4)$$

where  $r$  - distance from the pumping well to the observation well,

S - storativity, and

T - transmissivity.

Molz et al. also assume there are no head losses in the well nor any losses across the screen. They determined that the errors due to deviations from horizontal flow get larger as  $\Delta z_i$  gets smaller. However, they suggested hydraulic losses could generally be reduced or minimized by pumping at a rate just above the stall rate of the flowmeter.

There are a number of advantages to this method. First, all of the factors in Eq. (3-3) are easily determined. The effective well radius,  $r_w$ , and the storativity for each layer,  $S_i$ , are not needed in the calculation. This is helpful since both variables are usually



difficult, if not impossible, to precisely determine. However, the method still requires data from a fully penetrating pumping test to evaluate  $\bar{K}$ .

Molz et al. evaluated the variation in hydraulic conductivity with depth,  $K(z)$ , in three wells at a test site near Mobile, Alabama. They computed  $K(z)$  using Eqs. (3-2) and (3-3). The results of both equations followed identical trends. However, Eq. (3-2) reported higher values. The results were also compared to those from tracer and slug tests. All three test methods produced similar results in the overall nature and vertical distribution of hydraulic conductivity,  $K(z)$ . However, Molz et al. stated that the flowmeter test was the quickest and most convenient method for evaluating  $K(z)$ .

Molz et al. were also able to demonstrate that the flowmeter method is better able to detect layers of high hydraulic conductivity than the multi-slug approach. While the flowmeter produced results similar to those from the tracer test, the impeller meter data was more convenient to obtain. Molz et al. suggest that using the flowmeter test to obtain a  $K_i / \bar{K}$  profile and a pumping test to compute  $\bar{K}$  is a highly effective method for determining the horizontal hydraulic conductivity of individual layers.

Young (1995) reviewed different borehole flowmeter analysis methods. He also evaluated their applicability to a test site near Columbus, Mississippi composed of fluvial deposits. Aquifer and tracer testing at the site indicated that the aquifer is highly heterogeneous. Young used both the Cooper-Jacob and the  $K_i / \bar{K}$  profile (Molz et al., 1989) approaches to determine hydraulic conductivity ( $K$ ) from flowmeter test data. Trends in the hydraulic conductivity values were evaluated using results from geological investigations and from a large-scale, recirculating tracer test. The magnitude of  $K$  was

evaluated based on results from large-scale aquifer pumping tests and from small-scale tracer tests. The hydraulic conductivity values computed from the two flowmeter analyses were compared to the results of the pumping and tracer tests. Young's test results indicated that the different methods for analyzing flowmeter data produced significantly different values for hydraulic conductivity. It became apparent that the  $K_i / \bar{K}$  profile method was more appropriate based on the conditions encountered at the site. He was also able to demonstrate that borehole flowmeter data is effective for identifying regions of high-K deposits.

#### Analysis of Hydraulic Conductivity Using Flowmeter Data

Hanson and Nishikawa (1996) investigated using time-drawdown data combined with flowmeter data to estimate the vertical distribution of hydraulic conductivity in a layered aquifer system. Previous studies had used one method or the other, but not the two combined. The analyses were performed on test data from a complex, coastal, multilayer aquifer system near Oxnard, California. Data available from the site included: flowmeter test data, time-drawdown data, electric resistivity logs (e-logs), and lithologic logs. Flowmeter data is considered direct data, whereas the e-log data is considered indirect data.

Using analytical methods, Hanson and Nishikawa (1996) evaluated three conceptual models based on (1) flow-weighted discharge, (2) total discharge, and (3) e-log weighted discharge. Four conceptual models were examined with numerical models representing the  $K_i$  distribution based on: (1) e-log data including leakage from the aquitard layers, (2) flowmeter data including leakage, (3) strictly horizontal flow



aquifer layers, and (4) the direct flowmeter method of Molz et al. (1989), as shown in Eq. (3-3) presented earlier.

Hanson and Nishikawa estimated the bulk  $K$  value for the pumped and observation wells analytically using estimated pumping values apportioned vertically on the basis of measured flowmeter data and hydrostratigraphic interpretation of e-logs. A numerical groundwater model was used to estimate the  $K_i$  distribution using trial-and-error analysis.

In their study, the  $K_i$  distribution was estimated from flowmeter and aquifer test data for a long-screened production well in the lower aquifer system. These data were used to estimate the  $\bar{K}$  of the entire system and the  $K_i$  of specific layers. These data were also used in a numerical model to estimate the  $K_i$  of specific layers and to compare these with estimated from the indirect methods.

Both analytical and numerical models were used to evaluate the data. Analytical models included the Hantush solution and least-squares regression fit of the Theis and Cooper-Jacob methods. Hanson and Nishikawa used a groundwater modeling program called AX (Rutledge, 1991) for their numerical model. They used trial-and-error calibration in the numerical model. Numerical analyses were performed on two models: one based on e-log weighted data and one based on flowmeter data.

They found the hydraulic conductivity of individual layers,  $K_i$ , was overestimated by a factor of 4 or more when the flowmeter test data was not used. Also,  $\bar{K}$  in the simple analytical models was overestimated due to the release of water from aquitard storage. The  $K_i$  from the flowmeter weighted model was about twice as large as the values from the e-log weighted model. They were able to demonstrate that the e-log

model was able to match the time-drawdown data without matching the distribution of inflow at the well. The flowmeter model demonstrated that the time-drawdown data, as well as the distribution of inflow, could be matched. However, flowmeter resolution sensitivity is a problem in low permeability layers that contribute relatively little flow to the overall production.

The flowmeter provided additional layer information that is more cost effective compared to completing observations in the individual layers. Hanson and Nishikawa (1996) state that neither time-drawdown data nor flowmeter data alone can provide all the information needed to evaluate groundwater flow in layered systems. However, a combination of the two can recreate the measured drawdown, the distribution of wellbore flow, and a more realistic, conceptual model.

#### Hopscotch Algorithm

The Hopscotch method is a mixed explicit-implicit, finite-difference scheme used at alternating mesh points. According to Lapidus and Pinder, the concept was developed by Gordon (1965), and further refined by Gourlay (1970) and Gourlay and McGuire (1971). The general procedure for the scheme in one-dimensional space is as follows:

1. On any given row, calculate every other mesh point using a classic explicit approximation.
2. On the same row, calculate the missing points using a backwards implicit approximation.
3. On the next row, reverse the position of the explicit and implicit points.

In a three-dimensional space, the explicit points are calculated for a layer. Then, the implicit points are calculated using the explicit points. The overall results of the



## Chapter 4 - Groundwater Model Design

### General

The early stages of this research included the development of a groundwater model that used a mixed explicit-implicit algorithm. I investigated a finite-difference scheme called Hopscotch (Lapidus and Pinder, 1982). The authors claimed the Hopscotch method had the calculation ease of an explicit solution and the overall stability of an implicit solution. If this was true, it would allow me to develop a complete spreadsheet analysis for aquifer parameter identification. The following sections describe in more detail the Hopscotch algorithm, the development of my groundwater model, the testing of the model, and the results.

### Hopscotch Algorithm

The Hopscotch method is a mixed explicit-implicit, finite-difference scheme used at alternating mesh points. According to Lapidus and Pinder, the concept was developed by Gordon (1965), and further refined by Gourlay (1970) and Gourlay and McGuire (1971). The general procedure for the scheme in one-dimensional space is as follows:

1. On any given row, calculate every other mesh point using a classic explicit approximation.
2. On the same row, calculate the missing points using a backwards implicit approximation.
3. On the next row, reverse the position of the explicit and implicit points.

In a three-dimensional space, the explicit points are calculated for a layer. Then, the implicit points are calculated using the explicit points. The overall results of the

approximation are explicit, since there is only one unknown in any equation. Gordon showed the method to be stable and to be consistent with the model parabolic partial differential equation (PDE).

In development of the method, they started with the model parabolic PDE,

$$u_x = \mathcal{L} u + S(x, y_1, y_2), \quad (4-1)$$

where  $u$  - state variable of interest,

$\mathcal{L}$  - linear operator involving one, two, or three space terms ( $\partial^2/\partial y^2$ ),

$S$  - sink-source term that is a function of  $y_1$  and  $y_2$ ,

$x$  - nonspace variable, typically time, and

$y$  - space variables.

Replacing  $\mathcal{L}$  with any explicit or implicit solution form, Lapidus and Pinder developed the following equations to be used in an alternating fashion,

$$u_{r+1,s,t} = u_{r,s,t} + h \left( \frac{L}{k^2} u_{r,s,t} + S_{r,s,t} \right) \quad \text{and} \quad (4-2)$$

$$u_{r+1,s,t} = u_{r,s,t} + h \left( \frac{L}{k^2} u_{r+1,s,t} + S_{r+1,s,t} \right), \quad (4-3)$$

where  $L$  - a finite difference approximation of the linear operator,  $\mathcal{L}$ ,

$h$  - temporal discretization constant (e.g.,  $\Delta t$ ),

$k$  - spatial discretization constant (e.g.,  $\Delta y$ ), and

$r$ ,  $s$ , and  $t$  - mesh position indicators.

The explicit equation, Eq. (4-2), is used first for all points where  $(s+t)$  is even. Then, the implicit equation, Eq. (4-3), is used for the points where  $(s+t)$  is odd. As stated earlier, the positions of the explicit and implicit equations are then switched for each successive



step. Lapidus and Pinder defined the odd-even function  $\beta_{s,t}^r$ , where

$$\beta_{s,t}^r = 1 \quad \text{if } r+s+t \text{ is odd and} \quad (4-4)$$

$$\beta_{s,t}^r = 0 \quad \text{if } r+s+t \text{ is even.} \quad (4-5)$$

Using this function, the Hopscotch scheme can be written using a single equation,

$$u_{r+1,s,t} - h\beta_{s,t}^{r+1} \left( \frac{L}{k^2} u_{r+1,s,t} + S_{r+1,s,t} \right) = u_{r,s,t} + h\beta_{s,t}^r \left( \frac{L}{k^2} u_{r,s,t} + S_{r,s,t} \right). \quad (4-6)$$

Listed below are some of the advantages of this algorithm claimed by Lapidus and Pinder:

- The algorithm is unconditionally stable.
- Boundary conditions of various types can be included without major difficulty.
- It has minimal storage requirements since it allows for an overwrite of core storage.
- It is easy to program for both linear and nonlinear problems over general  $y_1$ - $y_2$  regions.
- It appears to handle problems in multiple space dimensions as well as those in one space dimension.
- The algorithm does not involve any tridiagonal solutions, making it much faster than other methods.

I was particularly interested in the algorithm's characteristic of being unconditionally stable. This advantage would have allowed me to develop a parameter identification package in a spreadsheet format, rather than traditional computer code.

Complete analysis in a spreadsheet format would have made the package more user-friendly.

### Model Development

To develop the algorithm for my groundwater model, I started with the governing equation for groundwater flow. I then derived the governing equation in terms of radial flow through a series of concentric shells. I then had an equation that I could state in explicit and implicit terms for my program.

Governing Equation. I started with the following groundwater governing equation for axi-symmetric flow in a layered aquifer:

$$K_r \left( \frac{\partial^2 h_i}{\partial r^2} + \frac{1}{r} \frac{\partial h_i}{\partial r} \right) + \frac{\partial}{\partial z} \left( K_v \frac{\partial h_i}{\partial z} \right) = Ss_i \frac{\partial h_i}{\partial t} + w_i \quad (4-7)$$

For my model, Eq. (4-7) is subject to the following boundary conditions:

$$(1) \quad \text{Limit}_{r \rightarrow 0} \quad 2\pi K_i r \frac{\partial h_i}{\partial r} = \frac{q_i}{\Delta z_i} \quad (4-8)$$

$$(2) \quad \text{Limit}_{r \rightarrow \infty} \quad h(r, z, t) = h_o \quad (4-9)$$

$$(3) \quad \text{Limit}_{t \rightarrow \infty} \quad h(r, z, t) = 0, \text{ and} \quad (4-10)$$

$$(4) \quad Q = \sum q_i \quad (4-11)$$

where  $K_r$  - horizontal hydraulic conductivity;

$K_v$  - vertical hydraulic conductivity;

$K_i$  - horizontal hydraulic conductivity for Layer i;

$h_i$  - head in Layer i as a function of r, z, and t;



$r$  - distance from the well to the observation point;

$z$  - depth;

$t$  - elapsed time;

$Ss_i$  - specific storage coefficient;

$w_i$  - volumetric source/sink rate;

$q_i$  - rate of groundwater flow in Layer  $i$ ; and

$\Delta z_i$  - thickness of Layer  $i$ .

The specific storage coefficient is the amount of water released from or taken into storage per unit volume of an aquifer per unit change in head. Storativity in an unconfined aquifer is equal to the specific storage coefficient times the aquifer or layer thickness.

Boundary Condition 1 states that immediately adjacent to the well, the flow in the layer equals the flow in the well. Boundary Condition 2 states that there is no change in head at some significantly large distance away from the well. Boundary Condition 3 states that the head will approach zero if pumping is continued indefinitely. Lastly, Boundary Condition 4 states that the total flow in the well equals the sum of flow in all the layers.

In axi-symmetric flow to a well, the flow occurs through a series of concentric shells. These shells decrease in area in the direction of the well. To model the flow through the differently-sized shells, the concept of hydraulic conductance was used. Hydraulic conductance,  $C$ , is defined as the hydraulic conductivity,  $K$ , multiplied by the area of flow,  $A$ , divided by the length of the flow path,  $L$ . Using conductance terms and Darcy's Law, I derived the governing equation in terms of an axi-symmetric mesh.

Radial Shell Balance. To model axi-symmetric flow, I conceptualized Darcy's Law in radial terms. Therefore, Darcy's Law, which states

$$Q = K_r A \frac{\partial h}{\partial r} \quad (4-12)$$

can be rewritten in radial terms as

$$Q = 2\pi r \Delta z K_r \frac{\partial h}{\partial r}, \quad (4-13)$$

where  $A$  is the cross-sectional area of flow, or  $2\pi r \Delta z$  in radial terms. Given the definition of hydraulic conductance, Eq. (4-13) can also be restated as

$$Q = C_r (dh), \quad (4-15)$$

where  $C_r = \frac{2\pi r \Delta z K_r}{dr} \quad (4-16)$

However, in axi-symmetric coordinates, the cross-sectional flow area is not constant in the lateral direction. Since each shell is small ( $dr$  thick), several shells in series can be used to define a compositional conductance,  $\overline{C}_r$ , where

$$\overline{C}_r = \frac{2\pi \Delta z K_r}{\ln(r)} \quad (4-17)$$

Using this compositional conductance, the flow can be rewritten as

$$Q = \overline{C}_r dh \quad (4-18)$$

Using Eqs. (4-17) and (4-18), I was able to calculate the radial shell balance. The horizontal (or radial) flows into and out of any shell,  $q_{in}$  and  $q_{out}$ , respectively, are determined using the following equations:

$$q_{in} = \frac{2\pi}{\ln(r_{i+1}/r_i)} K_r \Delta z_j (h_{i+1,j} - h_{i,j}) \quad \text{and} \quad (4-19)$$



$$q_{out} = \frac{2\pi}{\ln(r_i / r_{i-1})} K_r \Delta z_j (h_{i,j} - h_{i-1,j}), \quad (4-20)$$

where  $r_i$  is the distance to the node,  $i$  is the shell number, and  $j$  is the layer number.

In axi-symmetric flow to a well, there is an increase in the head gradient approaching the well due to the decrease in area. This changing gradient is more accurately modeled by using a closer spacing of the nodes adjacent to the well. Reilly and Harbaugh (1993) describe a method for developing an expanding mesh spacing. In this format, the distance from the well to each node is a multiple of the distance from the well to the node adjacent to the well. This spacing is given by

$$r_{i+1} = \alpha r_i \quad (4-21)$$

where  $r_i$  - radius to cell  $i$ ,

$r_{i+1}$  - radius to the next cell, and

$\alpha$  - the radius multiplication factor.

The distance from the center of the well to the center of the first node adjacent to the well is  $r_1$ ; and the distance to the center of node 2 is a multiple,  $\alpha$ , of  $r_1$ . Using this method of mesh spacing, Eqs. (4-19) and (4-20) become

$$q_{in} = \frac{2\pi}{\ln(\alpha)} K_r \Delta z_j (h_{i+1,j} - h_{i,j}) \quad \text{and} \quad (4-22)$$

$$q_{out} = \frac{2\pi}{\ln(\alpha)} K_r \Delta z_j (h_{i,j} - h_{i-1,j}). \quad (4-23)$$

Therefore, the flow into and out of a shell can be calculated independent of the lateral position of the shell.

Vertical Shell Balance. For the vertical shell balance, I again started with Darcy's Law, Eq. (4-12), to compute the vertical shell balance. The vertical area of flow for any shell,  $A_i$ , is computed by

$$A_i = \pi(r_{i+1/2}^2 - r_{i-1/2}^2). \quad (4-24)$$

However, since the  $r_i$  values are constant multipliers of each other,  $A_i$  can be written as

$$A_i = 2\pi r_i^2 \left( \frac{\alpha^2 - 1}{\alpha^2 + 1} \right). \quad (4-25)$$

Then by harmonic composition, the vertical flows into and out of the shell are computed using the following equations:

$$q_{in} = \frac{1}{\left( \frac{0.5\Delta z_{j-1}}{Kz_{j-1}A_i} + \frac{0.5\Delta z_j}{Kz_jA_i} \right)} (h_{i,j-1} - h_{i,j}) \quad \text{and} \quad (4-26)$$

$$q_{out} = \frac{1}{\left( \frac{0.5\Delta z_j}{Kz_jA_i} + \frac{0.5\Delta z_{j+1}}{Kz_{j+1}A_i} \right)} (h_{i,j} - h_{i,j+1}). \quad (4-27)$$

Storage Balance. The storativity of a shell,  $S_{i,j}$ , is computed by

$$S_{i,j} = A_i Ss_j \Delta z_i, \quad (4-28)$$

where  $A_i$  - conductance area given by Eq. (4-25) and

$Ss_j$  - specific storage coefficient for the layer.

By definition,  $Ss_j$  equals the specific yield,  $S_y$ , divided by the layer thickness,  $\Delta z_i$ .

Therefore,  $S_i$  can also be stated as

$$S_i = A_i S_y. \quad (4-29)$$



Model Algorithm. Combining Eqs (4-22), (4-23), (4-26), (4-27) and (4-28) gives

the governing equation in radial or axi-symmetric coordinate form,

$$2\pi K_r \Delta z_j \left[ \frac{h_{i+1,j} - h_{i,j}}{\ln(\alpha)} - \frac{h_{i,j} - h_{i-1,j}}{\ln(\alpha)} \right] + \quad (4-35)$$

$$\frac{1}{\frac{0.5\Delta z_j}{Kz_j A_i} + \frac{0.5\Delta z_{j+1}}{Kz_{j+1} A_i}} (h_{i,j+1} - h_{i,j}) - \frac{1}{\frac{0.5\Delta z_{j-1}}{Kz_{j-1} A_i} + \frac{0.5\Delta z_j}{Kz_j A_i}} (h_{i,j} - h_{i,j-1})$$

$$= A_i S s_j \Delta z_j \left[ \frac{h_{i,j}^{k+1} - h_{i,j}^k}{\Delta t} \right] + w_{i,j}. \quad (4-30)$$

The volumetric source/sink term,  $w_{i,j}$ , is equal to zero in all shells except for the shell adjacent to the well. In this first shell,  $w_{i,j}$  (or  $w_{i,1}$ ) represents the flow out of the innermost shell and is equal to the flow attributed to that layer,  $\Delta q_i$ .

To make the programming easier, I rewrote Eq. (4-30) using additional conductance terms,

$$a_i (h_{i+1,j} - 2h_{i,j} + h_{i-1,j}) + b_j (h_{i,j+1} - h_{i,j}) + c_j (h_{i,j-1} - h_{i,j}) \\ = d_{i,j} \left( \frac{h_{i,j}^{k+1} - h_{i,j}^k}{\Delta t} \right) + w_{i,j}, \quad (4-31)$$

where  $a_i = \frac{2\pi K_r \Delta z}{\ln(\alpha)}, \quad (4-32)$

$$b_j = \frac{1}{\frac{0.5\Delta z_j}{Kz_j A_i} + \frac{0.5\Delta z_{j+1}}{Kz_{j+1} A_i}}, \quad (4-33)$$

$$c_j = \frac{1}{\frac{0.5\Delta z_{j-1}}{Kz_{j-1}A_i} + \frac{0.5\Delta z_j}{Kz_jA_i}}, \text{ and} \quad (4-34)$$

$$d_{i,j} = A_i Ss_j \Delta z_i, \quad (4-35)$$

with  $a_i$ ,  $b_j$ ,  $c_j$ , and  $d_{i,j}$  as the conductance variables.

I now had the governing equation in the form I needed, and I was ready to test the Hopscotch algorithm.

Program Code. Figure 4-1 presents the flow chart for my Hopscotch program. The program begins by reading the input data file, initializing all constants, computing the conductance values, and initializing the time loop. For each time step, the head value is calculated using either an explicit or an implicit equation. The newly-calculated values are copied to the array of old values. Then, a new time step is begun and the process is repeated.

Six different versions of the explicit and implicit equations were developed. Due to variations in the flow conductance, separate equations were required for the top and bottom layers, the shell adjacent to the well, and the top and bottom corners of the first shell.

Input needed for the model included the following:

- the number of rows and shells (or columns),
- the radius to the first non-well cell and the radius multiplication factor,
- the initial water level in the well,
- the initial head in the aquifer,
- the length of the time step, number of time steps, and the time units,



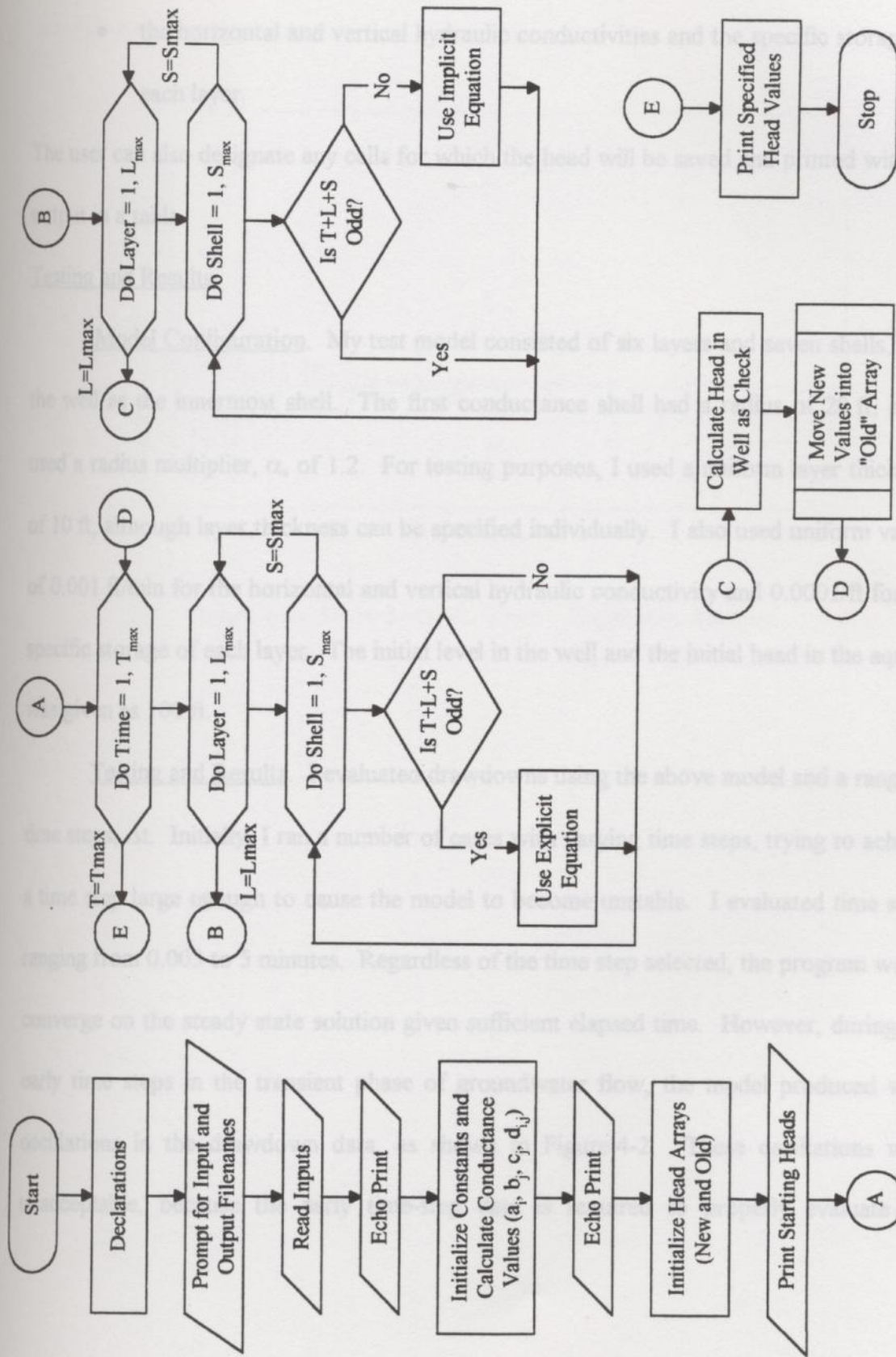


Figure 4-1: Hopscotch Model Flowchart

- the radius of the well, and
- the horizontal and vertical hydraulic conductivities and the specific storage for each layer.

The user can also designate any cells for which the head will be saved and printed with the output in a table.

### Testing and Results

Model Configuration. My test model consisted of six layers and seven shells, with the well as the innermost shell. The first conductance shell had a radius of 20 ft, and I used a radius multiplier,  $\alpha$ , of 1.2. For testing purposes, I used a uniform layer thickness of 10 ft, although layer thickness can be specified individually. I also used uniform values of 0.001 ft/min for the horizontal and vertical hydraulic conductivity and 0.0001/ft for the specific storage of each layer. The initial level in the well and the initial head in the aquifer was given as 100 ft.

Testing and Results. I evaluated drawdowns using the above model and a range of time steps,  $\Delta t$ . Initially, I ran a number of cases with varying time steps, trying to achieve a time step large enough to cause the model to become unstable. I evaluated time steps ranging from 0.003 to 5 minutes. Regardless of the time step selected, the program would converge on the steady state solution given sufficient elapsed time. However, during the early time steps in the transient phase of groundwater flow, the model produced wide oscillations in the drawdown data, as shown in Figure 4-2. These oscillations were unacceptable, because the early time-step data is required to properly evaluate the



storativity of the layer or aquifer. Therefore, I had to abandon this model for another groundwater-flow modeling tool.

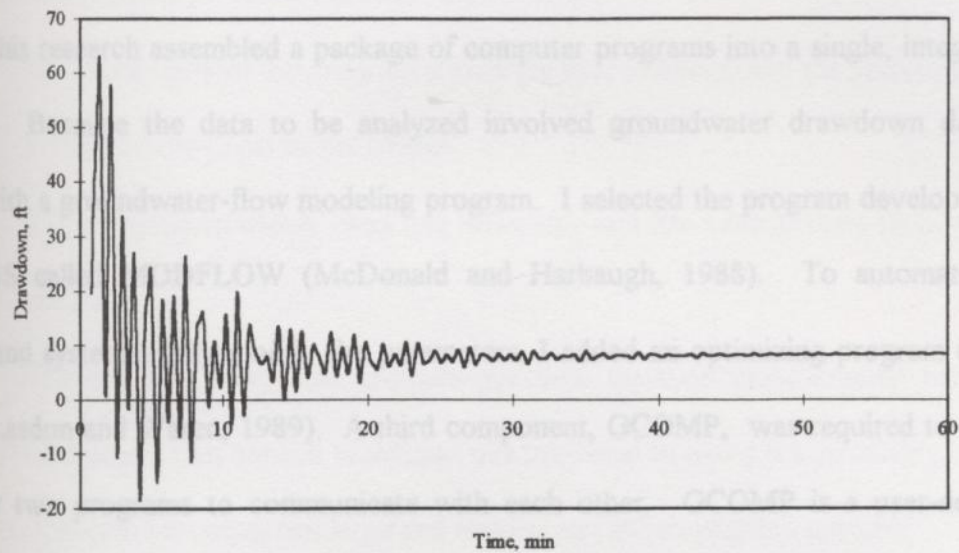


**Figure 4-2: Drawdown vs. Time - Hopscotch Analysis**

## Chapter 5 - General Approach

### General

This research assembled a package of computer programs into a single, integrated program. Because the data to be analyzed involved groundwater drawdown data, I started with a groundwater-flow modeling program. I selected the program developed by the USGS called MODFLOW (McDonald and Harbaugh, 1988). To automate the analysis and systematically modify the parameters, I added an optimizing program called GRG2 (Lasdon and Waren, 1989). A third component, GCOMP, was required to allow the other two programs to communicate with each other. GCOMP is a user-defined subroutine of GRG2. MODFLOW was revised to be called as a subroutine to GCOMP. All three components were written in FORTRAN source code. A more detailed discussion of each of these components is presented below.

### Groundwater Modeling Program

The program MODFLOW uses a modular finite-difference model to simulate groundwater flow in an aquifer. The program consists of a main program and a series of highly independent subroutines called "modules." The modules are grouped in packages with each package dealing with a specific hydrological feature or linear solution technique. The hydrological packages simulate the effects of wells, recharge, rivers, drains, evapotranspiration, and general head boundaries. The modularity of the program allows the user to select the packages that are applicable to the specific conditions being analyzed. Applicable packages are called and the other packages will be ignored. The



program was designed with modules to allow for the maximum flexibility. The program can be used for two- or three-dimensional models.

I selected MODFLOW for the following reasons:

- The modularity of the program allows the user to select only the packages that are applicable to his or her model.
- The program is widely used and accepted, and has been proven to be fairly accurate.
- The program solves the groundwater flow equation using implicit solution techniques. An implicit technique was preferred to avoid the possibility of the time step becoming too large and making an explicit solution unstable.
- The model simulates flow in three directions. Vertical flow is ignored in many models.
- The program is relatively efficient with respect to computer memory and execution time. The execution time is important since the optimizing program, while varying the parameters, will call the groundwater modeling program numerous times.

In MODFLOW, groundwater flow is simulated using a block-centered, finite-difference approach. The continuous system is replaced by a finite set of points in space and time, and the partial derivatives in the generalized flow equation are replaced by finite-differences approximations. This setup leads to a system of linear algebraic (or quasi-linear) difference equations that are solved simultaneously.

The user divides each layer of the system into rows and columns. This creates a grid of cells, defined by their layer, row, and column. The hydraulic properties are specified by the user for each cell, and the program assumes these properties to be generally uniform over the area of the cell. Figure 5-1 presents a drawing of the MODFLOW physical model.

The hydraulic properties required are transmissivity, storativity, and vertical hydraulic conductivity. Transmissivity, comprised of the horizontal hydraulic conductivity,  $k_i$ , times the layer thickness,  $\Delta z_i$ , is used as input, rather than using the two parameters separately.

The width of each set of rows and columns,  $\Delta x$  and  $\Delta y$  respectively, are also specified by the user. Additional input used in the analyses consisted of: boundary conditions, starting head conditions, the pumping rate (or stress event), and iteration parameters.

MODFLOW evaluates the head in each cell using the following equation,

$$\begin{aligned}
 & CR_{i,j-1/2,k}(h_{i,j-1,k}^m - h_{i,j,k}^m) + CR_{i,j+1/2,k}(h_{i,j+1,k}^m - h_{i,j,k}^m) + CC_{i-1/2,j,k}(h_{i-1,j,k}^m - h_{i,j,k}^m) \\
 & + CC_{i+1/2,j,k}(h_{i+1,j,k}^m - h_{i,j,k}^m) + CV_{i,j,k-1/2}(h_{i,j,k-1}^m - h_{i,j,k}^m) + \\
 & CV_{i,j,k+1/2}(h_{i,j,k+1}^m - h_{i,j,k}^m) + P_{i,j,k}(h_{i,j,k}^m) + Q_{i,j,k} = \\
 & SS_{i,j,k}(\Delta y_i \Delta x_j \Delta z_k) \frac{(h_{i,j,k}^m - h_{i,j,k}^{m-1})}{(t_m - t_{m-1})}, \quad (5-1)
 \end{aligned}$$

where CR, CC, CV - the conductance flow through a row, column, or layer face;

or, product of the hydraulic conductivity and the cross-sectional area of flow divided by the length of the flowpath;



$h^m$  - head at time step  $m$ ;

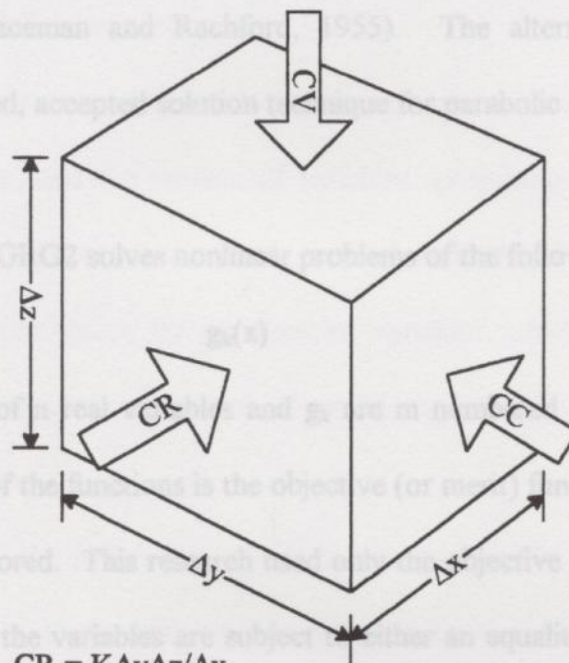
$P$  - outside flow factor that is dependent of head;

$Q$  - outside flow factor that is independent of head;

$SS$  - specific storage coefficient; and

$t$  - time.

An equation in the form of Eq. (5-1) is written for each variable head cell and the system is solved simultaneously for head at the next time step. Figure 5-1 presents a diagram showing the flow cell dimensions and the conductance directions.



$$CR = K\Delta y\Delta z/\Delta x$$

$$CC = K\Delta x\Delta z/\Delta y$$

$$CV = K\Delta x\Delta y/\Delta z$$

**Figure 5-1: MODFLOW Conductance Diagram**

The model uses an iterative approach to obtain the solution. The head at the end of the time step is assigned an estimated value, based on the values at the start of the time

step. Heads are then calculated across the grid changing the estimated values and producing a new set of values that more closely fit the system of equations. The process is repeated until the changes produced are smaller than a user-defined tolerance or a maximum number of iterations have been performed.

The program uses a backward-difference approach to prevent mathematical instability during the calculation of heads. The finite-difference equations can be solved using either a strongly implicit procedure or slice-successive overrelaxation. I used the strongly implicit procedure in my analyses, which is similar to the alternating-direction implicit method (Peaceman and Rachford, 1955). The alternating-direction implicit method is a well-tested, accepted solution technique for parabolic systems.

#### Optimizer Program

The program GRG2 solves nonlinear problems of the following form,

$$\text{Minimize } g_k(\mathbf{x}) \quad (5-2)$$

where  $\mathbf{x}$  is a vector of  $n$  real variables and  $g_k$  are  $m$  numbered real, linear or nonlinear functions of  $\mathbf{x}$ . One of the functions is the objective (or merit) function, and the others are constraints or are ignored. This research used only the objective function. The objective function and each of the variables are subject to either an equality, inequality, or bounds constraint.

The program attempts to solve problems of this form by the Generalized Reduced Gradient Method. The GRG2 program uses the first partial derivatives of the function  $g_k$  with respect to each variable  $x_i$ . These derivatives are estimated by finite-difference



approximation. Either a forward- or central-difference solution can be used; the forward difference method was used for this research.

The GRG2 program was selected because the generalized reduced gradient algorithm is an efficient and accepted nonlinear programming technique. This specific version of the algorithm attempts to return to the constraint surface at each step, which results in a more stable algorithm (Lasdon et al., 1978).

The user is required to prepare a subroutine called GCOMP. This subroutine computes the values of  $\mathbf{g} = \mathbf{g}_1, \dots, \mathbf{g}_m$  for any given vector  $\mathbf{x}$ . This subroutine is discussed in more detail in the following section.

For input, the user must define the number of constraint functions, one of which is the objective function, and the number of variables comprising the  $\mathbf{x}$  vector. The user must also specify the constraints that apply to the functions and variables. The input file also includes the initial values for the  $\mathbf{x}$ -vector variables. Additional input consists of selection of the computation method (forward- or central-difference) and various optimization parameters.

After reading the initial data, the program operates in two phases. A phase I optimization is started if the initial points supplied by the user do not satisfy all the constraints on the function vector,  $\mathbf{g}$ . This phase terminates with either a feasible solution or a message that the problem is unfeasible. The phase II begins with the feasible solution, and attempts to optimize the objective function by adjusting the values of the variables in the  $\mathbf{x}$  vector.

The GRG2 algorithm solves Eq. (5-2) by solving a series of reduced problems. These reduced problems are solved using a gradient method. The GRG2 program solves for the basic variables in terms of the nonbasic variables. Then, the objective function is rewritten in terms of these basic and nonbasic variables. The revised function (the Lagrangian function in basic variables) is called  $F(x)$ . A search direction is determined from the gradient of  $F(x)$  and a one-dimensional search is performed to minimize  $F(x)$ . A variation of Newton's method is used to solve the system of basic variables.

#### Processor Program

A processor or translator subroutine, called GCOMP, is required to allow the MODFLOW and GRG2 programs to communicate with each other. The GCOMP component is a user-supplied subroutine to GRG2 and makes the subroutine calls to MODFLOW. The GCOMP subroutine takes the current  $x$  vector from GRG2, and computes and returns the objective function. In these analyses, the variables comprising the  $x$  vector consisted of the three aquifer parameters for each layer: storativity, transmissivity, and vertical hydraulic conductivity. Figure 5-2 shows the structure of the GCOMP subroutine.

GCOMP performs the following steps:

- Receives the initial or current values of the aquifer parameters (the  $x$  vector) from GRG2.
- Creates the MODFLOW input file that contains the aquifer parameter information using the above values.
- Calls MODFLOW to calculate model heads or drawdowns.



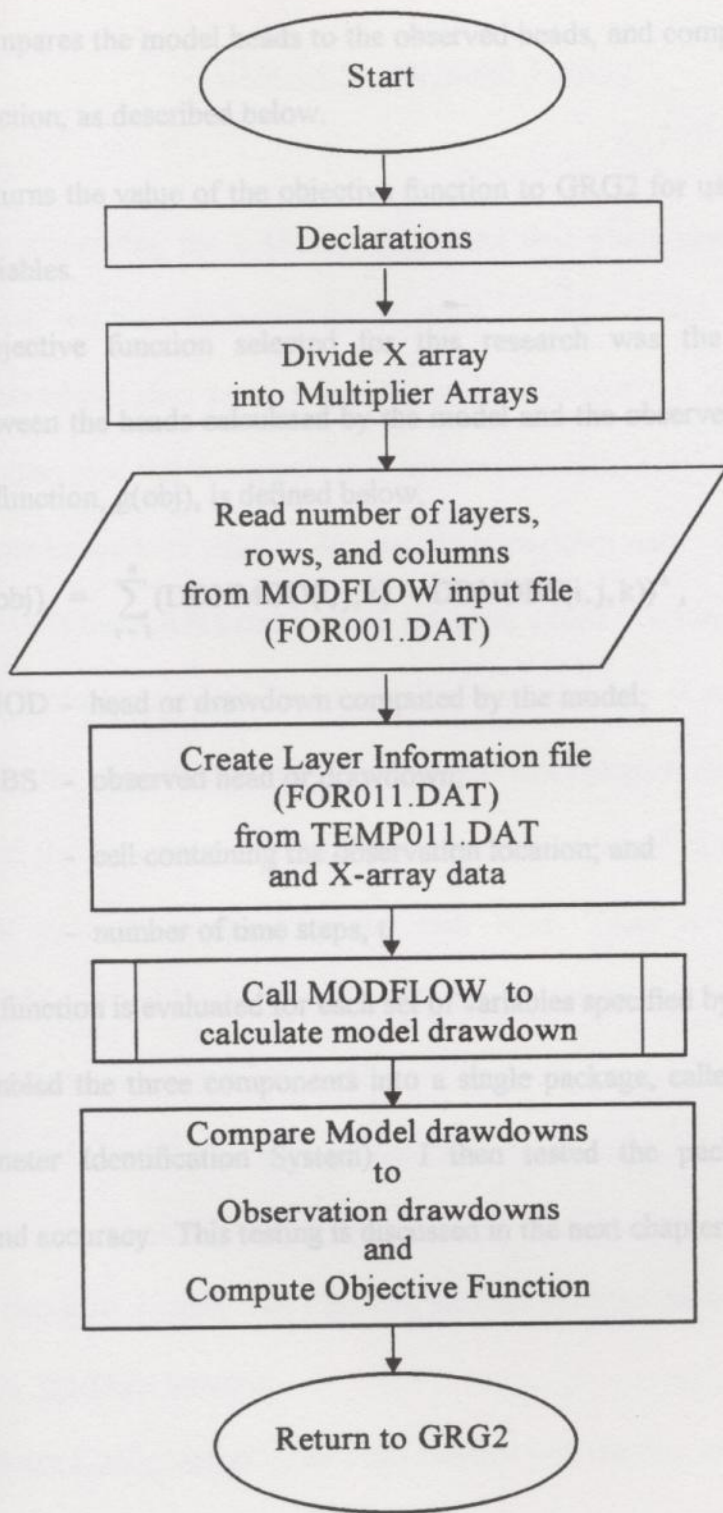


**Figure 5-2: GCOMP Flowchart**

- Compares the model heads to the observed heads, and computes the objective function, as described below.
- Returns the value of the objective function to GRG2 for use in modifying the variables.

The objective function selected for this research was the sum of squared differences between the heads calculated by the model and the observed heads over time. This objective function,  $g(obj)$ , is defined below,

$$g(obj) = \sum_{t=1}^n (DDNMOD(i, j, k) - DDNOBS(i, j, k))^2, \quad (5-3)$$

where DDNMOD - head or drawdown computed by the model;

DDNOBS - observed head or drawdown;

$i, j, k$  - cell containing the observation location; and

$n$  - number of time steps,  $t$ .

This objective function is evaluated for each set of variables specified by GRG2.

I assembled the three components into a single package, called LAPIS (Layered Aquifer Parameter Identification System). I then tested the package to verify its functionality and accuracy. This testing is discussed in the next chapter.



## Chapter 6 - Package Testing

### Methodology

After assembling the LAPIS package, the next phase was testing the package against known solutions to verify its accuracy. I started with simple aquifers, and developed drawdown data using spreadsheets that modeled the analytical (i.e., known) solutions. I then used this drawdown data as the observation data. I created a set of input files using the parameters used to develop the drawdown data. I then ran the LAPIS package to verify that LAPIS could return the same values. To further test the package, I varied the individual parameters to determine how much larger or smaller the values could be relative to the actual values and the program still compute the correct answer. As stated earlier, the parameters used in this research consisted of storativity, transmissivity, and vertical hydraulic conductivity for each layer. There is no vertical hydraulic conductivity for the last layer. Therefore, the number of variables for any analysis equals one less than three times the number of layers.

I selected two well-known and widely-accepted analytical solutions to use in my testing. I used the Theis solution to model a single-layer aquifer and the Hantush solution to model a two-layer system. The following sections describe these analyses.

### Testing using the Theis Solution

Problem Configuration. The Theis solution was the first mathematical analysis of transient drawdown in a confined aquifer. This equation was developed for a single-layer aquifer. Therefore, only two variables were evaluated in this set of analyses - storativity and transmissivity. Figure 6-1 presents the typical configuration for this solution.

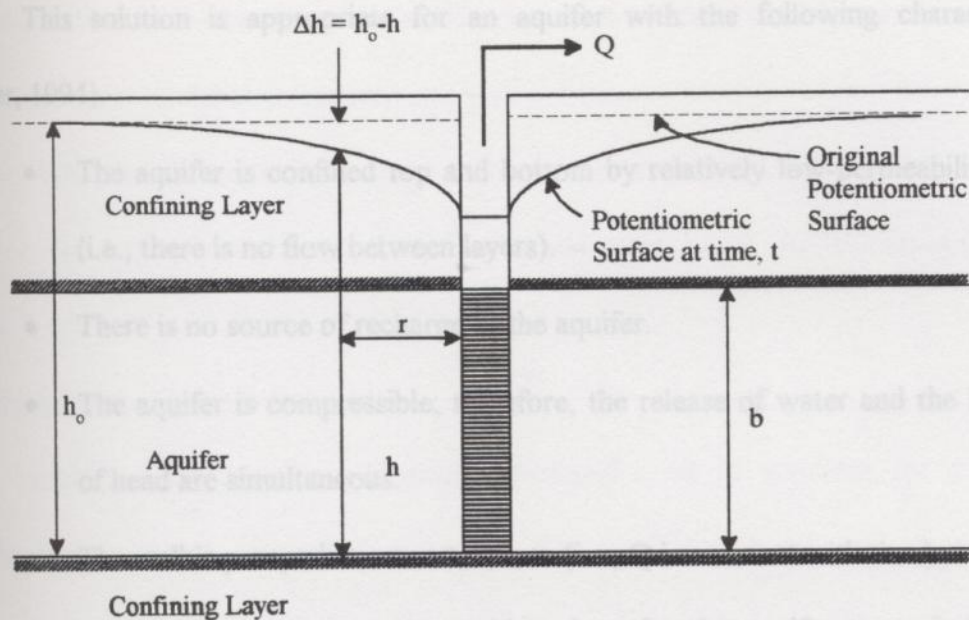


**Figure 6-2: Aquifer Configuration - Theis Solution**

The Theis solution (Fetter, 1994) solves for drawdown using the following equations:

$$\Delta h = \frac{Q}{4 \pi T} \int_u^{\infty} \frac{e^{-u}}{u} du \quad \text{and} \quad (6-1)$$

$$u = \frac{r^2 S}{4 T t}, \quad (6-2)$$

where  $\Delta h$  - change in head or drawdown,

$Q$  - pumping rate,

$T$  - aquifer transmissivity, or the thickness of the aquifer times its horizontal permeability,

$r$  - radial distance from the pumping well to the observation well,

$S$  - aquifer storativity, and

$t$  - elapsed time since pumping began.



This solution is appropriate for an aquifer with the following characteristics (Fetter, 1994).

- The aquifer is confined top and bottom by relatively low-permeability layers (i.e., there is no flow between layers).
- There is no source of recharge to the aquifer.
- The aquifer is compressible; therefore, the release of water and the lowering of head are simultaneous.
- The well is pumped at a constant rate (i.e.,  $Q$  is constant with time).

After selecting common or reasonable values for the aquifer transmissivity and storativity, the distance from the observation well to the pumping well, and the pumping rate, I calculated the drawdown over time using a spreadsheet that modeled the Theis solution to simulate the response. These head values became the observation data for comparison. Input for the LAPIS package then was developed for this aquifer. For the first analysis, the same values used to develop the observation data were used as input. I performed this analysis to verify that the LAPIS package was working properly. Then, I increased or decreased the value of the two parameters. I then fixed the transmissivity, and made additional analyses varying only the storativity value.

Results. Varying both the storativity and transmissivity, the program was able to return the "correct" or actual parameters from initial values that were ten times larger to 20 times smaller (a multiplier of 0.05). I did not make additional runs to determine how much larger or smaller the parameters would have to be before the LAPIS package was unable to return the actual values. In these analyses, the computed storativity value for

each run did not vary much from the input value. This indicates the relative insensitivity of the groundwater model to storativity.

When the transmissivity was set at the actual values, the LAPIS package was able to return the actual value for storativity from initial values of  $10^{-5}$  to  $10^{+4}$  times the actual value.

### Testing using the Hantush Solution

**Problem Configuration.** Hantush developed a set of solutions for a confined aquifer with a source of vertical recharge. The vertical recharge can come from an aquitard above, or below the aquifer providing a favorable hydraulic gradient. This recharge factor added another variable to my analysis, for a total of three variables that were evaluated. Figure 6-2 presents the typical configuration for the Hantush solution.

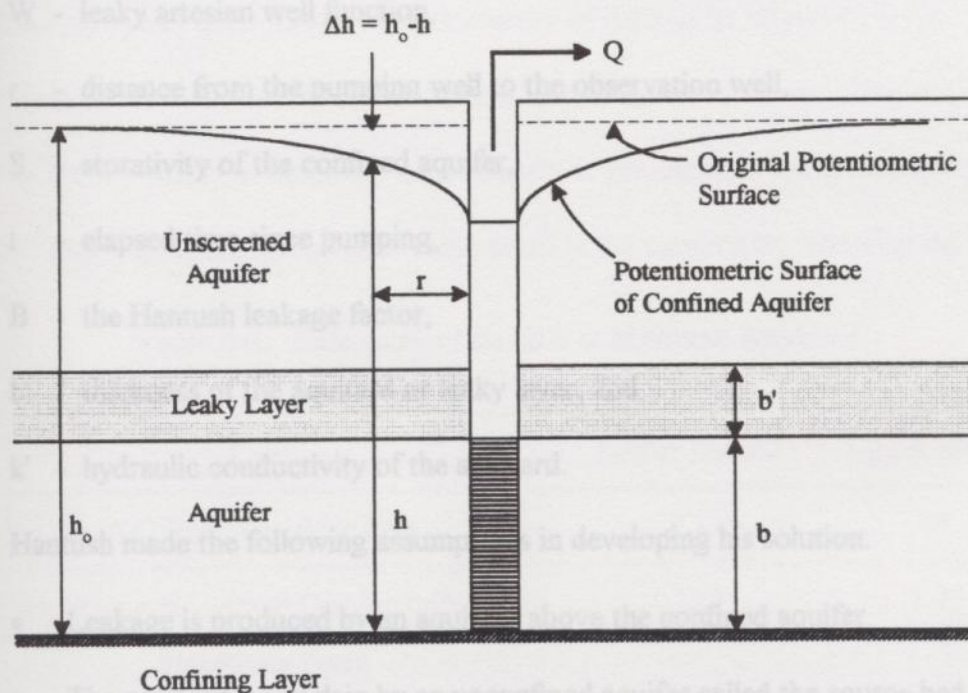


**Figure 6-2: Aquifer Configuration - Hantush Solution**



The Hantush solution evaluates drawdown in a confined aquifer with or without leakage or drains from the aquifer other than from the pumping well (Fetter, 1994). The Hantush solution is

$$\Delta h = \frac{Q}{4\pi T} W(u, r/B) = \frac{Q}{4\pi T} \int_u^\infty \frac{e^{-u - \frac{r^2}{4B^2u}}}{u} du, \quad (6-3)$$

$$u = \frac{r^2 S}{4Tt}, \text{ and} \quad (6-4)$$

$$B = (Tb'/K')^{1/2}, \quad (6-5)$$

where  $\Delta h$  - drawdown in the confined aquifer,

$Q$  - pumping rate,

$T$  - transmissivity of the confined aquifer,

$W$  - leaky artesian well function,

$r$  - distance from the pumping well to the observation well,

$S$  - storativity of the confined aquifer,

$t$  - elapsed time since pumping,

$B$  - the Hantush leakage factor,

$b'$  - thickness of the aquitard or leaky layer, and

$k'$  - hydraulic conductivity of the aquitard.

Hantush made the following assumptions in developing his solution:

- Leakage is produced by an aquitard above the confined aquifer.
- The aquitard is overlain by an unconfined aquifer called the source bed.
- The water table in the source bed is initially horizontal.

- The water table in the source bed does not fall during pumping of the aquifer. This produces a constant gradient of flow from the aquitard to the aquifer.
- Groundwater flow in the aquitard is vertical.
- The aquifer is compressible; therefore, the release of water and the lowering of head is simultaneous.
- The aquitard is incompressible; therefore, no water is released from storage in the aquitard during pumping in the aquifer.

In the testing, I used a two-layer model with leakage from the first layer (i.e., the aquitard) into the second layer, or confined aquifer. This model resulted in three variables to be evaluated by the LAPIS package, resulting in an increased number of variable used in testing. The three variables consisted of: vertical conductivity from the aquitard layer to the aquifer layer, and transmissivity and storativity of the aquifer layer.

Results. I evaluated the performance of the LAPIS package using the Hantush model with three cases. A summary of the results is presented in the table below. These cases and their results are discussed in more detail in the paragraphs following the table.

**Table 6-1: Summary of Results of Hantush Analyses**

	Case	Lower Bound	Upper Bound
1	All Three Variables Free	0.3	5*
2	Horizontal and Vertical Conductivity Free, Storativity Fixed	0.125	3.75
3	Storativity Free, Horizontal and Vertical Conductivity fixed	$10^{-7}$ *	$10^{+4}$ *

\* Limit of the analyses.



I started the analyses, Case 1, by allowing all three variables to vary. The LAPIS package was able to "find" the correct values for the horizontal and vertical conductivities starting from a lower bound of 0.3 times the original values (or 3.3 times smaller) to an upper bound of at least five times the original values. I did not investigate any values larger than five times the original values. However, due to the insensitivity of the groundwater modeling program, the computed values for storativity generally did not vary much from the initially provided value. storativity was evaluated. I also found that the

For Case 2, I fixed the storativity value at the observation value and allowed the horizontal and vertical conductivities to vary. For this case, the lower boundary increased to 0.125 times the original values. However, the upper limit decreased to 3.75 times the original value.

For the runs discussed above, initial values for both conductivities were varied in the same direction; both variables were either larger or smaller than the original. I also performed a few analyses to evaluate the results if one conductivity was larger and one was smaller than the original values. The LAPIS package was unable to return the correct value for either conductivity in this case.

As stated earlier, the storativity value was not optimized in Case 1 where all variables were evaluated by the LAPIS package. For Case 3, I fixed the two conductivities at their original values and allow the LAPIS package to evaluate the storativity variable. I evaluated storativity values from  $10^{-7}$  to  $10^{+4}$  times larger than the original value. Regardless of the initial value, the package was able to return the original value for storativity when the conductivities were fixed at their original values.

## Findings

## Chapter 7 - Data Analysis

The LAPIS package provided good agreement with the analytical cases. There is a fairly wide range of initial values provided to the program where the original or "correct" values could be returned. However, the optimizer does have its limits. Therefore, the user must start with a reasonable estimate of the parameters. Optimization of the storativity was better accomplished when the values for both horizontal and vertical conductivities were fixed and only the storativity was evaluated. I also found that the more variables the problem contains, the better the estimate of initial values needs to be.

As discussed earlier in Chapter 5, Hanson and Nishikawa (1989) used data from an aquifer test site northwest of Los Angeles, California in their study. The USGS provided me with some of the same data used by Hanson and Nishikawa. This data included flowmeter data from the pumping well and time-drawdown data from two of the four observation wells at the site. The USGS also provided data from an electric resistivity test performed in the pumping well. Additional information about the site and aquifer was taken from Hanson and Nishikawa. They used the data to evaluate the vertical distribution of hydraulic conductivity using trial-and-error methods and an explicit-in-time, finite-difference model, called AX (Ruffedge, 1991). I hoped to improve on their analysis methods by using an automated package that included an optimizer algorithm.

The aquifer test site consists of a 36-square mile subbasin located northwest of Los Angeles in Pleasant Valley. According to the USGS, the geology of the complex aquifer system has been divided into an upper system and a lower system as shown in Figure 7-1.



## Chapter 7 - Data Analysis

### General

After establishing the validity of the LAPIS package, I then used it to evaluate actual field data. In this chapter, I will discuss: the aquifer test site and the data provided for testing, the development of the groundwater model, the evaluation of the hydraulic properties of the site using the LAPIS package, and the results of this testing.

### Description of Field Data

As discussed earlier in Chapter 3, Hanson and Nishikawa (1996) used data from an aquifer test site northwest of Los Angeles, California for their study. The USGS provided me with some of the same data used by Hanson and Nishikawa. This data included flowmeter data from the pumping well and time-drawdown data from two of the four observation wells at the site. The USGS also provided data from an electric resistivity test performed in the pumping well. Additional information about the site and aquifer was taken from Hanson and Nishikawa. They used the data to evaluate the vertical distribution of hydraulic conductivity using trial-and-error methods and an explicit-in-time, finite-difference model, called AX (Rutledge, 1991). I hoped to improve on their analysis methods by using an automated package that included an optimizer algorithm.

The aquifer test site consists of a 36-square mile subbasin located northwest of Los Angeles in Pleasant Valley. According to the USGS, the geology of the complex aquifer system has been divided into an upper system and a lower system as shown in Figure 7-1.

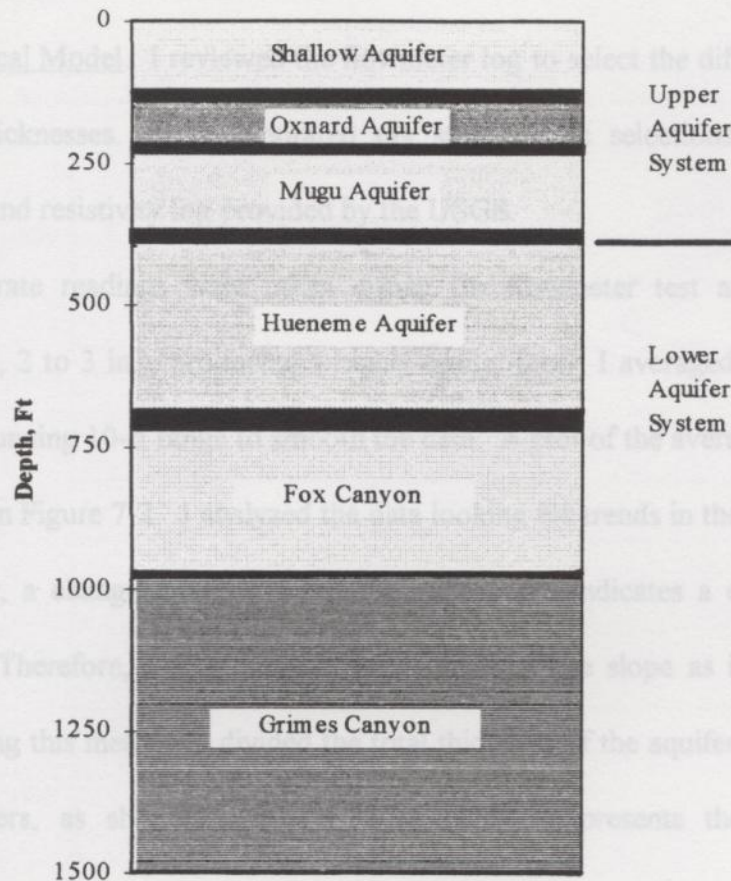


**Figure 7-1: Site Geology**

The upper system consists of relatively flat-lying alluvial deposits are about 400-ft thick. The lower system consists of more than 1,000 ft of folded and faulted fluvial and shallow marine deposits. Drilling data show the fluvial deposits consist of alternating beds of sand and clay about 5- to 50-ft thick, and the marine deposits consist of fine-grained sand and silt beds more than 100-ft thick that are separated by silt and clay beds that are as much as 50-ft thick. Formations in the upper and lower aquifer systems are unconformably overlain with subregionally extensive, basal aquifer layers that are relatively large contributors of water in production wells screened over large intervals.



## Model Configuration

Physical Model. I reviewed the flowmeter log to select the different aquifer layers and their thicknesses. I corroborated my stratigraphic selections with the geology information and resistivity log provided by the USGS.

Spin-rate readings were taken during the flowmeter test at very small depth intervals (i.e., 2 to 3 in.), producing a highly erratic plot. I averaged the raw flowmeter data over a running 10-ft range to smooth the data. A plot of the averaged flowmeter data is presented in Figure 7-2. I analyzed the data looking for trends in the average slope. As stated earlier, a change in the average slope generally indicates a change in hydraulic conditions. Therefore, I used any change in the average slope as indicator of a layer change. Using this method, I divided the total thickness of the aquifer system, B, into six different layers, as shown in Figure 7-2. Table 7-1 presents the layers and their thicknesses.

**Table 7-1: Layer Information**

Layer	Depth Range (ft)	Thickness, $\Delta z_i$ (ft)
1	390-670	280
2	670-690	20
3	690-830	140
4	830-920	90
5	920-1160	240
6	1160-1400	240

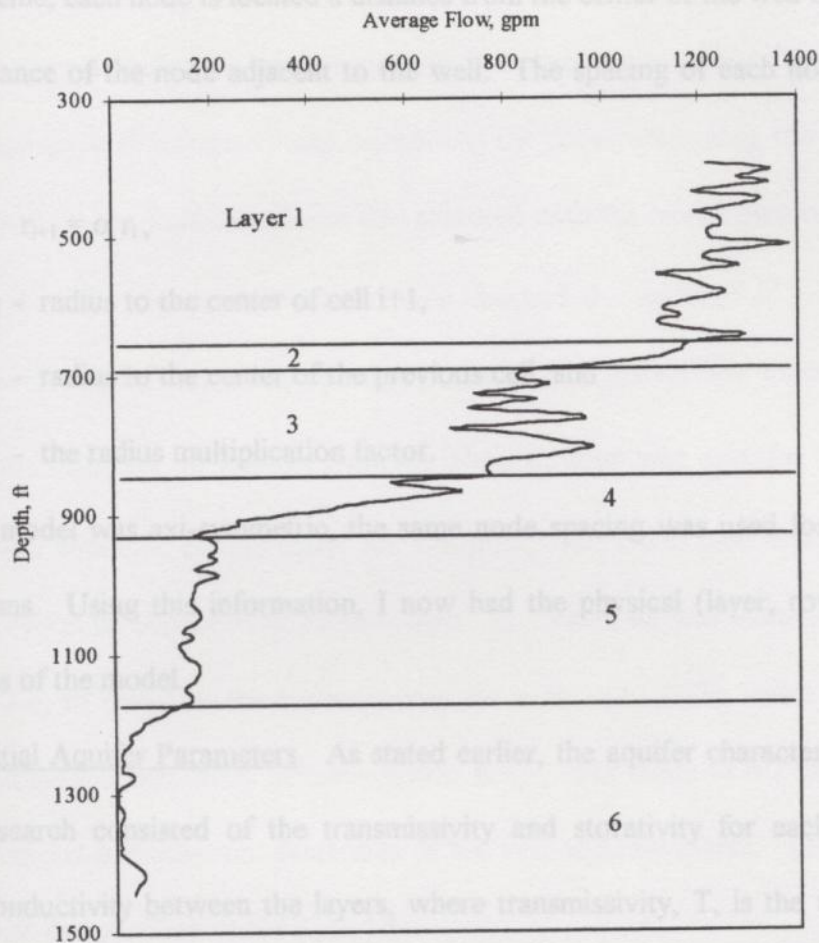


**Figure 7-2: Flowmeter Data**

I was provided time-drawdown data from two of the four observation wells at the site. One set of data was taken in a well screened from 800- to 860-ft depth; this data is from my Layer 3. The second well was screened from 938- to 998-ft depth, which falls within Layer 5.

I selected the horizontal grid (row and column spacing) of each layer based on the location of the observations wells relative to the pumping well. I used the radial, expanding mesh grid as described in Reilly and Harbaugh (1993) and earlier in Chapter 4.



In this scheme, each node is located a distance from the center of the well that is a multiple of the distance of the node adjacent to the well. The spacing of each node is calculated using

$$r_{i+1} = \alpha r_i, \quad (7-1)$$

where  $r_{i+1}$  - radius to the center of cell  $i+1$ ,

$r_i$  - radius to the center of the previous cell, and

$\alpha$  - the radius multiplication factor.

Since my model was axi-symmetric, the same node spacing was used for both the rows and columns. Using this information, I now had the physical (layer, row, and column) dimensions of the model.

Initial Aquifer Parameters. As stated earlier, the aquifer characteristics optimized in this research consisted of the transmissivity and storativity for each layer and the vertical conductivity between the layers, where transmissivity,  $T$ , is the thickness of the layer,  $\Delta z_i$ , times its horizontal hydraulic conductivity,  $K_i$ . The initial horizontal hydraulic conductivity of each layer,  $K_i$ , was evaluated using the method proposed by Molz et al. (1989), where  $K_i$  is given by

$$K_i = \bar{K} \left( \frac{\Delta Q_i / \Delta z_i}{QP / B} \right). \quad (7-2)$$

The contribution of flow by each layer,  $\Delta Q_i$ , was determined from analysis of the flowmeter log. The difference in flow rates at the top and bottom of a layer is equivalent to the amount of flow contributed by that layer,  $\Delta Q_i$ . The total discharge from the well,  $QP$ , was given in the data. The individual layer thicknesses,  $\Delta z_i$ , and the total aquifer thickness,  $B$ , were determined as described earlier.

The bulk hydraulic conductivity,  $\bar{K}$ , was computed by modeling the aquifer as a single layer using a Theis type-curve approach. This method consists of varying the values for transmissivity and storativity and calculating the drawdown using the Theis solution, Eqs. (6-1) and (6-2). This calculation was repeated until the model time-drawdown curve matched that of the observation data. I then checked the value of  $\bar{K}$  using the LAPIS package developed for this research. Again, the aquifer system was modeled as a single layer, and the value for  $\bar{K}$  derived from the Theis solution was used for the initial input. Once the bulk hydraulic conductivity,  $\bar{K}$ , was computed, I was then able to compute the horizontal hydraulic conductivity of each layer,  $K_i$ . Then,  $K_i$  was multiplied by the layer thickness,  $\Delta z_i$ , to compute the transmissivity for each layer. The initial estimate of the vertical hydraulic conductivity between layers,  $K_{v,i+1}$ , was taken as 0.1 times the average of the horizontal hydraulic conductivities of the two adjacent layers. Table 7-2 presents the results of the calculations for  $K_i$  and  $T$ .

The 20-ft thickness of Layer 2 is small relative to the other layers. However, as can be seen from Table 7-2, Layer 2 contributes almost 20 percent of the flow into the well. I analyzed two separate cases, merging Layer 2 with either Layer 1 or Layer 3. In either case, LAPIS was unable to adequately model the observed time-drawdown data. Although the thickness of Layer 2 is only 2 percent of the total thickness, the flow into the well from this zone is too significant for this zone not to be designated as a separate layer.



Table 7-2: Transmissivity Calculations

Layer	Depth (ft)	Thickness, $\Delta z_i$ (ft)	Average Flow Rate (gpm)	Flow Rate for Layer, $\Delta Q_i$		$K_i/\bar{K}$	$K_i$ (ft/min)	Transmis- sivity, T (ft <sup>2</sup> /min)
				(gpm)	(ft <sup>3</sup> /min)			
	390		1278.65					
1		280		128.4	17.2	0.36	3.28E-03	0.919
	670		1150.25					
2		20		240.75	32.2	9.57	8.61E-02	1.722
	690		909.5					
3		140		115	15.4	0.65	5.88E-03	0.823
	830		794.5					
4		90		607.25	81.2	5.36	4.83E-02	4.344
	920		187.25					
5		240		32.1	4.3	0.11	9.57E-04	0.230
	1160		155.15					
6		240		147.15	19.7	0.49	4.39E-03	1.053
	1400		8					
<b>Totals:</b>	<b>B =</b>	<b>1010</b>	<b>QP =</b>	<b>1270.65</b>	<b>169.85</b>			

Note:  $\bar{K} = 0.009$  ft/min.

Storativity,  $S$ , of a confined aquifer of layer is equal to the specific storage coefficient times the thickness of the aquifer or layer. The specific storage coefficient,  $S_s$ , for each layer was estimated using (Marsily, 1986)

$$S_s = \rho \omega g \left( \beta_1 - \beta_s + \frac{\alpha}{\omega} \right), \quad (7-3)$$

where  $\rho$  - mass per unit volume or density,

$\omega$  - porosity,

$g$  - acceleration due to gravity,

$\beta_1$  - compressibility of the liquid,

$\beta_s$  - compressibility of the solid, and

$\alpha$  - compressibility coefficient of the porous medium.

In this case, the compressibility coefficient,  $\alpha$ , is the compressibility of the soil matrix. The specific storage coefficient,  $S_s$ , is primarily a function of the porosity,  $\omega$ , and soil compressibility. The unit weight,  $\gamma$  or  $\rho g$ , varied only slightly relative to  $\omega$  and  $\alpha$  for the materials involved. Typically, the solid is assumed to be incompressible; therefore,  $\beta_s$  was neglected. These factors reduce Eq. (7-3) to the following:

$$S_s = \gamma \omega \left( \beta_1 + \frac{\alpha}{\omega} \right). \quad (7-4)$$

Marsily (1986) lists ranges of values for  $\alpha$  for different soil types. An average value was selected due to the small overall range of values ( $10^{-6}$  to  $10^{-8}$  Pa<sup>-1</sup>). I also selected average values for  $\gamma$  and  $\beta_1$ . Then, I computed  $S_s$  for values of  $\omega$  ranging from 0.3 to 0.7. These values for  $S_s$  varied by only  $1.2 \times 10^{-6}$ ; therefore, I started with an average value of



$6.0 \times 10^{-5} \text{ ft}^{-1}$  for the specific storage coefficient. The initial estimate of storativity for each layer,  $S_i$ , was then computed by multiplying  $S_s$  by  $\Delta z_i$ .

Once I had initial estimates for transmissivity, storativity, and vertical hydraulic conductivity for each layer, I was able to complete my input files. The data structure for the aquifer parameters in MODFLOW consists of one array for each variable in each layer. The first line of each array contains a constant; every element in the array is multiplied by this constant. For my research, I assumed that each layer was homogeneous and isotropic. Therefore, every cell in an array had the same value for any variable. These array constants were the variables in the  $\mathbf{x}$ -vector in GRG2. The optimizer program then varied these constants. This approach simplified the programming, since only a one number was changed for each array, rather than each element in the array. Therefore, the terms "variable" and "formation constant" are interchangeable in the discussion of this research.

The structure of the observation data was also reviewed and the GCOMP code was revised so that the correct observations were compared. I was then ready to start my analyses.

(Case 4)

In Case 5, I only allowed the  $K_v$  constants from the observation layers (3 and 5) and the applicable  $K_{v(i,j)}$  constants to vary; all other  $K_v$ ,  $K_{v(i,j)}$ , and  $S_i$  constants were fixed at 1.0. Case 6 completed the analysis of Case 5, by optimizing the storativity constants for layers 3 and 5.

Case 7 was a variation of Case 2. In these three analyses, I fixed the  $S_i$  constants at different values to see what, if any, effect the value of these constants had on the final values of the  $K_v$  and  $K_{v(i,j)}$  constants.

## Testing

Overall, I had 17 variables: one  $K_i$  constant and  $S_i$  constant for each layer, and five  $Kv_{i,i+1}$  constants. As stated earlier, I only had observation data in Layers 3 and 5. As described in Chapter 5, the optimizer program allows the user to either fix the value of each of the variables or allow them to be varied by GRG2. Table 7-3 summarizes the different cases I analyzed.

For my first case, I allowed all 17 variables to vary (i.e., the variables were "free" to vary, as opposed to fixed). For the next case, I allowed only the  $K_i$  and  $S_i$  variables for the observation layers and the applicable  $Kv_{i,i+1}$  variables to vary; the other variables were fixed at their initial values.

In Case 3, I fixed the  $S_i$  constants at 1.0 and allowed all of the  $K_i$  and  $Kv_{i,i+1}$  constants to vary. I ran this case based on the results of my model calibration studies, which found the groundwater program is less sensitive to storativity than it is to the two hydraulic conductivity factors. I then fixed the values of the  $K_i$  and  $Kv_{i,i+1}$  constants at the values determined from Case 3 and allowed LAPIS to optimize only the  $S_i$  values (Case 4).

In Case 5, I only allowed the  $K_i$  constants from the observation layers (3 and 5) and the applicable  $Kv_{i,i+1}$  constants to vary; all other  $K_i$ ,  $Kv_{i,i+1}$ , and  $S_i$  constants were fixed at 1.0. Case 6 completed the analysis of Case 5, by optimizing the storativity constants for Layers 3 and 5.

Case 7 was a variation of Case 2. In these three analyses, I fixed the  $S_i$  constants at different values to see what, if any, effect the value of these constants had on the final values of the  $K_i$  and  $Kv_{i,i+1}$  constants.



**Table 7-3: Summary of Test Cases**

Case	Description
1	All 17 variables free to vary.
2	Only $K_i$ and $S_i$ variables in observation layers and applicable $K_{v_{i,i+1}}$ variables free; all others fixed.
3	All $K_i$ and $K_{v_{i,i+1}}$ variables were free; all $S_i$ constants were fixed at 1.0.
4	All $S_i$ variables were free; $K_i$ and $K_{v_{i,i+1}}$ values fixed to those from Case 3.
5	Only applicable $K_i$ and $K_{v_{i,i+1}}$ variables free; all other variables fixed.
6	Only $S_3$ and $S_5$ variables were free; all other $S_i$ variables fixed at 1.0. $K_i$ and $K_{v_{i,i+1}}$ values fixed to those from Case 5.
7a	All $K_i$ and $K_{v_{i,i+1}}$ variables free; $S_i$ constants fixed at $10^{-4}$ (Variation of Case 2).
7b	All $K_i$ and $K_{v_{i,i+1}}$ variables free; $S_i$ constants fixed at $10^{-6}$ (Variation of Cases 2 and 7a).
7c	All $K_i$ and $K_{v_{i,i+1}}$ variables free; $S_i$ constants fixed at $10^{-2}$ (Variation of Cases 2, 7a, and 7b).

Results or analysis by Hanson and Mishikawa (1996) are also presented for comparison.

Overall, allowing all 17 variables to vary (Case 1) produced the best match of model time-drawdown data to the observation data. The results of Case 1 are presented in Table 7-4. I calculated the root-mean-square error (RMS Error) and the average relative error for the Layers 3 and 5 data using

$$\text{RMS Error} = \sqrt{\frac{1}{n} \sum (\text{Observed} - \text{Model})^2} \quad \text{and} \quad (7-5)$$

$$\text{Ave. Relative Error} = \frac{1}{n} \sum (\text{Observed} - \text{Model}) / \text{Observed}, \quad (7-6)$$

where  $n$  is the number of data. The results of the LAPIS package have a RMS error of 1.1 and an average relative error of 0.37 for the Layer 3 data. The Layer 5 data have a RMS error of 0.9 and an average relative error of 0.23.

The procedure of fixing the  $S_i$  constants and varying only the  $K_i$  and  $K_{V_{i,i+1}}$  constants, then fixing the  $K_i$  and  $K_{V_{i,i+1}}$  constants and optimizing the  $S_i$  variables did not produce as accurate results as it did during model testing with fabricated data. This result is likely because of the larger number of variables involved in the analysis.

However, fixing the  $S_i$  constants at different values had little effect on the computed values of the  $K_i$  and  $K_{V_{i,i+1}}$  variables, even though the time-drawdown data varied significantly. As stated earlier, these results illustrate the insensitivity of the groundwater model to storativity.

Figures 7-3 and 7-4 present plots of the observation data along with the time-drawdown data for Cases 1 and 7c analyses for Layers 3 and 5, respectively. The remaining cases produced unsatisfactory results. The time-drawdown data from the



flowmeter analysis by Hanson and Nishikawa (1996) are also presented for comparison.

Tables 7-5 and 7-6 present the initial estimates and the computed values for the three

aquifer parameters analyzed.

Table 7-4: Results of the Case 1 Analysis

Parameter	Initial Value	Final Value
$K_1$ (ft/min)	3.21E-03	5.66E-03
$K_2$ (ft/min)	85.0E-03	22.7E-03
$K_3$ (ft/min)	5.71E-03	4.97E-03
$K_4$ (ft/min)	47.8E-03	6.81E-03
$K_5$ (ft/min)	1.04E-03	1.61E-03
$K_6$ (ft/min)	3.75E-03	0.79E-03
$S_1$	17.0E-03	0.223
$S_2$	1.20E-03	1.20E-07
$S_3$	8.40E-03	1.34E-04
$S_4$	5.40E-03	5.40E-07
$S_5$	14.0E-03	14.0E-07
$S_6$	3.00E-03	3.00E-07
$Kv_{1,2}$ (ft/min)	1.00E-02	1.00E-06
$Kv_{2,3}$ (ft/min)	1.30E-02	1.30E-06
$Kv_{3,4}$ (ft/min)	2.60E-02	2.10E-02
$Kv_{4,5}$ (ft/min)	2.30E-02	2.19E-02
$Kv_{5,6}$ (ft/min)	8.60E-02	6.59E-02

**Table 7-4: Results of the Case 1 Analysis**

Parameter	Initial Value	Final Value
$K_1$ (ft/min)	3.21E-03	5.66E-03
$K_2$ (ft/min)	85.0E-03	22.7E-03
$K_3$ (ft/min)	5.71E-03	4.97E-03
$K_4$ (ft/min)	47.8E-03	0.81E-03
$K_5$ (ft/min)	1.04E-03	1.61E-03
$K_6$ (ft/min)	3.75E-03	0.79E-03
$S_1$	17.0E-03	0.222
$S_2$	1.20E-03	1.20E-07
$S_3$	8.40E-03	1.34E-04
$S_4$	5.40E-03	5.40E-07
$S_5$	14.0E-03	14.0E-07
$S_6$	3.00E-03	3.00E-07
$Kv_{1,2}$ (ft/min)	1.00E-02	1.00E-06
$Kv_{2,3}$ (ft/min)	1.30E-02	1.30E-06
$Kv_{3,4}$ (ft/min)	2.60E-02	2.10E-02
$Kv_{4,5}$ (ft/min)	2.30E-02	2.19E-02
$Kv_{5,6}$ (ft/min)	0.60E-02	0.59E-02



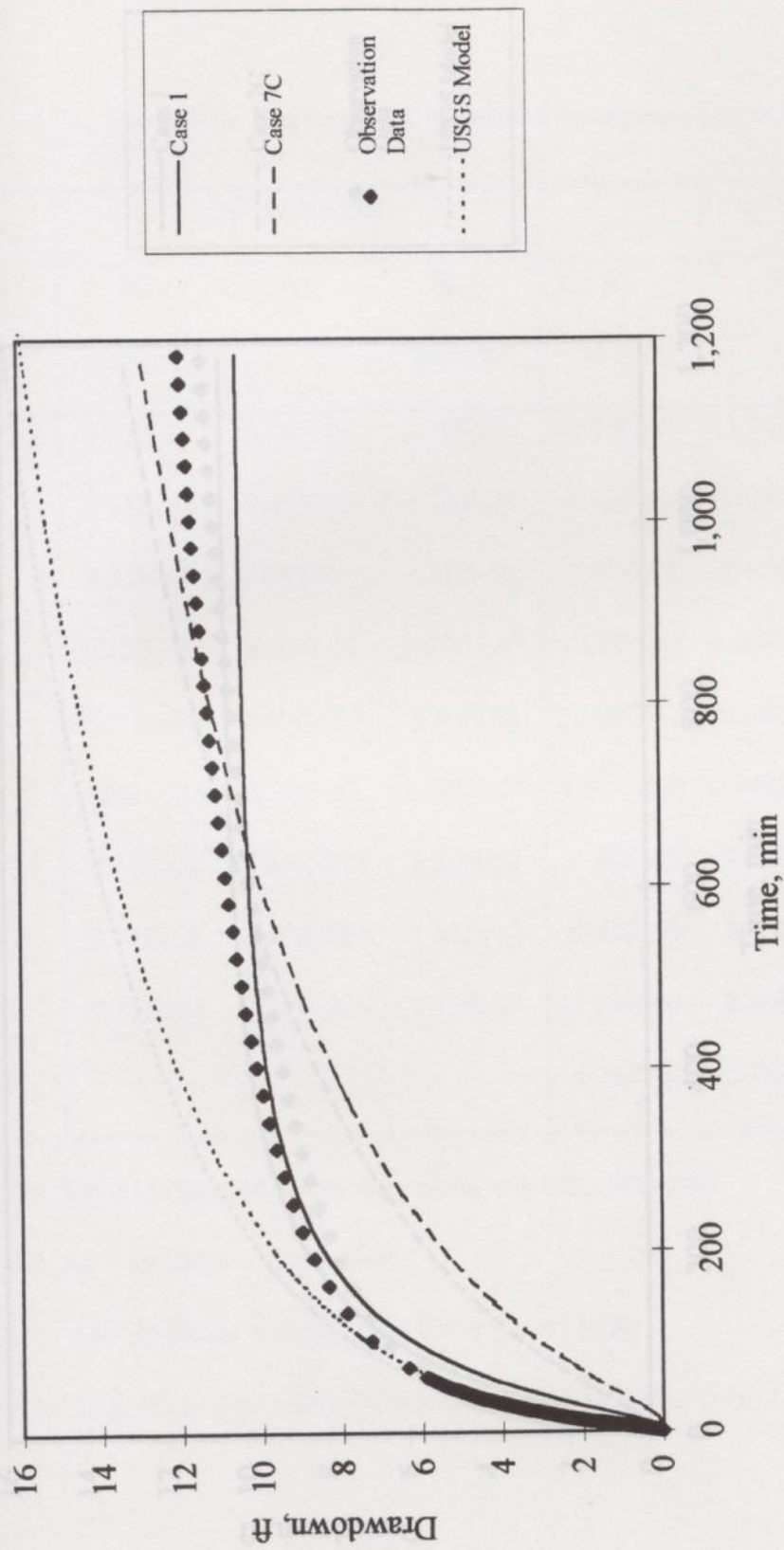


Figure 7-3: Drawdown vs. Time - Layer 3

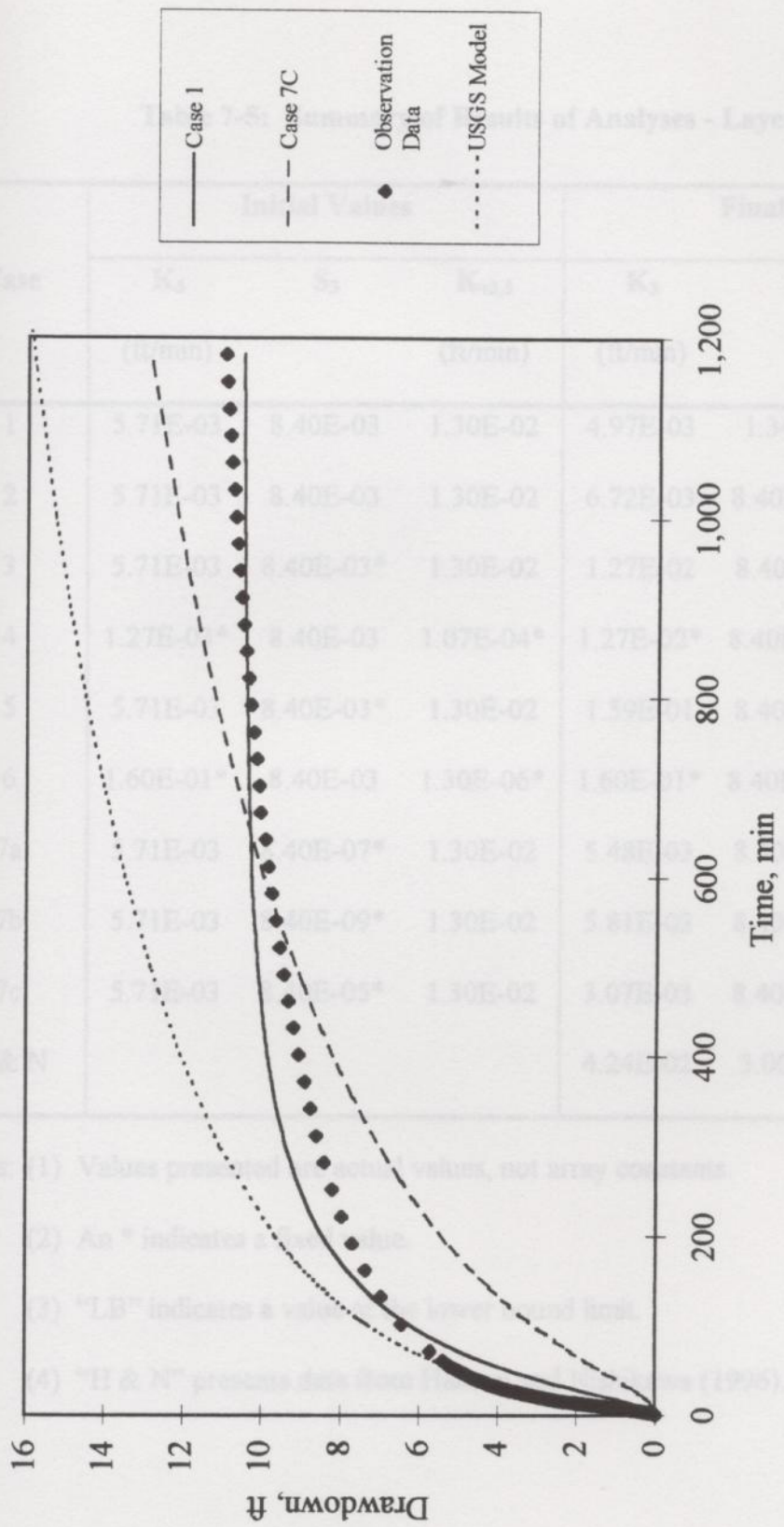


Figure 7-4: Drawdown vs. Time - Layer 5



Table 7-5: Summary of Results of Analyses - Layer 3

Case	Initial Values			Final Values		
	$K_3$ (ft/min)	$S_3$	$K_{v2,3}$ (ft/min)	$K_3$ (ft/min)	$S_3$	$K_{v2,3}$ (ft/min)
1	5.71E-03	8.40E-03	1.30E-02	4.97E-03	1.34E-04	1.30E-06 <sup>LB</sup>
2	5.71E-03	8.40E-03	1.30E-02	6.72E-03	8.40E-07 <sup>LB</sup>	1.30E-06 <sup>LB</sup>
3	5.71E-03	8.40E-03*	1.30E-02	1.27E-02	8.40E-03*	1.07E-04
4	1.27E-03*	8.40E-03	1.07E-04*	1.27E-02*	8.40E-09 <sup>LB</sup>	1.07E-04*
5	5.71E-03	8.40E-03*	1.30E-02	1.59E-01	8.40E-03*	1.30E-06 <sup>LB</sup>
6	1.60E-01*	8.40E-03	1.30E-06*	1.60E-01*	8.40E-07 <sup>LB</sup>	1.30E-06*
7a	5.71E-03	8.40E-07*	1.30E-02	5.48E-03	8.40E-07*	1.30E-02
7b	5.71E-03	8.40E-09*	1.30E-02	5.81E-03	8.40E-09*	1.30E-02
7c	5.71E-03	8.40E-05*	1.30E-02	3.07E-03	8.40E-05*	1.30E-02
H & N				4.24E-02	3.00E-04	

Notes: (1) Values presented are actual values, not array constants.

(2) An \* indicates a fixed value.

(3) "LB" indicates a value at the lower bound limit.

(4) "H & N" presents data from Hanson and Nishikawa (1996).

Conclusions

Table 7-6: Summary of Results of Analyses - Layer 5

Case	Initial Values			Final Values		
	$K_5$ (ft/min)	$S_5$	$K_{v4,5}$ (ft/min)	$K_5$ (ft/min)	$S_5$	$K_{v4,5}$ (ft/min)
1	1.04E-03	1.40E-02	2.30E-02	1.61E-03	1.40E-06 <sup>LB</sup>	2.19E-02
2	1.04E-03	1.40E-02	2.30E-02	1.04E-07	1.40E-06 <sup>LB</sup>	7.69E-01
3	1.04E-03	1.40E-02*	2.30E-02	8.52E-04	1.40E-02*	3.69E-02
4	8.52E-04*	1.40E-02	3.69E-02*	8.52E-04*	2.28E-05	3.69E-02*
5	1.04E-03	1.40E-02*	2.30E-02	7.11E-06	1.40E-02*	3.61E-02
6	7.11E-06*	1.40E-02	3.61E-02*	7.11E-06*	1.40E-06 <sup>LB</sup>	3.61E-02*
7a	1.04E-03	1.40E-06*	2.30E-02	1.03E-03	1.40E-06*	2.30E-02
7b	1.04E-03	1.40E-08*	2.30E-02	1.05E-03	1.40E-08*	2.30E-02
7c	1.04E-03	1.40E-04*	2.30E-02	9.61E-04	1.40E-04*	2.30E-02
H & N				9.03E-03	3.15E-04	

Notes: (1) Values presented are actual values, not array constants.

(2) An \* indicates a fixed value.

(3) "LB" indicates a value at the lower bound limit.

(4) "H & N" presents data from Hanson and Nishikawa (1996).



## Chapter 8 - Conclusions and Recommendations

### Conclusions

Through calibration testing, I found the results from the LAPIS package to have good agreement with analytical cases. Therefore, I determined that package was valid for purposes of this research. I was also able to automate the inverse analysis of aquifer parameters, saving the time and effort of the user.

The use of optimizer program allows for a logical, rather than random, approach to modifying the parameters. A logical approach is more important as the number of layers (and therefore variables) increases.

It has been proven previously that flowmeter data provide a detailed record of the vertical distribution of flow into a well or borehole. I have shown that these data are very valuable for (1) identifying layers of different hydraulic characteristics, and (2) estimating the horizontal hydraulic conductivity of individual layers. The use of flowmeter data improves the inverse analysis of parameters in a layered system.

### Recommendations for Further Study

Additional research is required to determine if there is a limitation to the number of variables, and therefore layers, the LAPIS package can evaluate and still produce acceptable results.

The groundwater flow model in the LAPIS package could be changed, and another program that is more sensitive to storativity be used. However, this change would require all new calibration and testing. A generic optimization algorithm, such as simulated annealing, could be used instead of GRG2. Simulated annealing does not rely on gradient

information. Therefore, in principle, it could find solutions in cases where the model response is relatively insensitive to a parameter. However, simulated annealing and similar approaches require very fast simulations.

In this research, I optimized the aquifer parameters by comparing model drawdowns to observed drawdowns. I also assumed that any flow in a layer was into the well, which is not always the case. Another approach would be to let the groundwater model compute the flow of the individual layers and compare this information to that from a flowmeter test. This approach would better address any layers with flow from the well back into the layer.

The package was developed and tested using a UNIX-based workstation. It would be helpful to use the package on different platforms to compare accuracy and speed performance. The performance of the package would be related to the processor platform and the amount of working memory. Different computer configurations will, at least, have different speed performances.



## References

- Capuano, R.M. and Jan, R.Z. (1996), "In situ hydraulic conductivity of clay and silty-clay fluvial-deltaic sediments, Texas Gulf Coast," Ground Water, Vol. 34, No. 3, pp. 545-551.
- Daniel, D.E. (1984), "Predicting hydraulic conductivity of clay liners," ASCE Journal of Geotechnical Engineering, Vol. 113, No. 7, pp. 766-799.
- Elsbury, B.R., Daniel, D.E., Sraders, G.A. and Anderson, D.C. (1990), "Lessons learned from compacted clay liner," ASCE Journal of Geotechnical Engineering, Vol. 116, No. 11, pp. 1641-1660.
- Fetter, C.W. (1994), Applied Hydrogeology, Macmillan College Publishing Co., New York, 654 pp.
- Gourlay, A.R. (1970), "Hopscotch: A fast second-order partial differential equation solver," J. Inst. Math. Appl., Vol. 6, pp. 375-390.
- Gourlay, A.R. and McGuire, G.R. (1971), "General Hopscotch algorithm for the numerical solution of partial differential equations," J. Inst. Math. Appl., Vol. 7, pp. 216-227.
- Hanson, R.T. and Nishikawa, T. (1996), "Combined use of flowmeter and time-drawdown data to estimate hydraulic conductivities in layered aquifer systems," Ground Water, Vol. 34, No. 1, pp. 84-94.
- Hill, M.C. and Zheng, C. (1995), "Progress Made in Groundwater Flow and Transport Modeling," EOS, Transactions, American Geophysical Union, Vol. 76, No. 40, pp. 393-394.

- Lapidus, L. and Pinder, G.F. (1982), Numerical Solution of Partial Differential Equations in Science and Engineering, John Wiley & Sons, New York, 677 pp.
- Lasdon, L.S., Waren, A.D., Jain, A., and Ratner, M. (1978), "Design and testing of a generalized reduced gradient code for nonlinear programming," ACM Transactions on Mathematical Software, Vol. 4, No. 1, pp. 34-50.
- Lasdon, L.S. and Waren, A.D. (1989), GRG2 User's Guide, Department of Management Science and Information Systems, University of Texas at Austin, Austin, Texas.
- Marsily, G. de (1986), Quantitative Hydrogeology, Academic Press, San Diego, 440 pp.
- McDonald, M.G. and Harbaugh, A.W. (1988), "A modular three-dimensional finite-difference ground-water flow model," U.S. Geological Survey Techniques of Water Resources Investigations, Book 6, Chapter A1.
- Molz, F.J., Morin, .RH., Hess, A.E., Melville, J.G., and Güven, O. (1989), "The impeller meter for measuring aquifer permeability variations: evaluation and comparison with other tests," Water Resources Research, Vol. 25, No. 7, pp. 1677-1683.
- Peaceman, D.W. and Rachford, H.H. (1955), "The numerical solution of parabolic and elliptic differential equations," SIAM Journal, Vol. 3, pp. 28-41.
- Reilly, T.E. and Harbaugh, A.W. (1993), "Simulation of cylindrical flow to a well using the U.S. Geological Survey modular finite-difference ground-water flow model," Ground Water, Vol. 31, No. 3, pp. 489-494.
- Rutledge, A.T. (1991), "An axisymmetric finite-difference flow model to simulate drawdown in and around a pumped well," Water Resources Investigations, Report No. 90-4098, U.S. Geological Survey, 33 pp.



Wang, H.F. and Anderson, M.P. (1982), Introduction to Groundwater Modeling,

W.H. Freeman & Company, San Francisco, 237 pp.

Yeh, W.W-G. (1986), "Review of parameter identification procedures in groundwater

hydrology: the inverse problem," Water Resources Research, Vol. 22, No. 2,

pp. 95-108.

Young, S.C. (1995), "Characterization of high-K pathways by borehole flowmeter and

tracer tests," Ground Water, Vol. 33, No. 2 , pp. 311-318.

## Bibliography

- Avriel, M. (1976), Nonlinear Programming: Analysis and Methods, Prentice-Hall, New Jersey, 512 pp.
- Bear, J. (1979), Hydraulics of Groundwater, McGraw-Hill, New York, 569 pp.
- Bear, J. And Verruijt, A. (1987), Modeling Groundwater Flow and Pollution, D. Reidel, Dordrecht, Holland, 420 pp.
- Hayward, A.T.J. (1979), Flowmeters: A Basic Guide and Source-Book for Users, MacMillan Press, Ltd, London, 197 pp.
- Huyakorn, P.S. and Pinder, G.F. (1983), Computational Methods in Subsurface Flow, Academic Press, New York, 473 pp.
- Log Interpretation Principles/Applications, Schlumberger Education Services, Houston, Texas (1989).
- Neuman, S.P. and Narasimhan, T.N. (1977), "Mixed explicit-implicit iterative finite element scheme for diffusion-type problems," International Journal for Numerical Methods in Engineering, Vol. 11, pp. 309-323.
- Pandit, A. and Abi Aoun, J.M. (1994), "Numerical modeling of axis-symmetric flow," Ground Water, Vol. 32, No. 3 (May-June), pp. 458-464.
- Pinsky, M.A. (1991) Partial Differential Equations and Boundary Value Problems with Applications, 2nd Ed., McGraw-Hill, New York, 461 pp.
- Ponzini, G., Crosta, G. and Giudici, M. (1989), "Identification of thermal conductivities by temperature gradient profiles: one-dimensional steady flow," Geophysics, Vol. 54, No. 5 (May), pp. 643-653.



Reilly, T.E. (1984), "A Galerkin finite-element flow model to predict the transient response of a radially symmetric aquifer," Water-Supply Paper 2198, U.S. Geological Survey, 13 pp.

Szikely, F. (1995), "Estimation of unsteady, three-dimensional drawdown in single, vertically heterogeneous aquifers," Ground Water, Vol. 33, No. 4, (July-Aug.) pp. 669-674.

## APPENDIX

GCOMP Source Code and

Sample Input

SUBROUTINE GCOMPNG.JQ

C

C PAMELA G. ANDERSON, AUGUST 14, 1995

C

C Date Description

C

C 8/14/95 PGA Creation of MODFLOW data file written and checked

C 8/28/95 PGA Conversion to subroutine and addition of MODFLOW call

C 9/20/95 PGA Added UCI for second constraint

C 9/23/95 PGA Added first loop so that data from all time steps

C 9/25/95 PGA Changed order of variable to allow for any effect on UCI

C

C 10/20/95 PGA Added section reading observation data for model data specific cells

C (Note: program reads SPECIFIC cells, range for different data )<gc3.D>

C 11/20/95 PGA Revised observation data for multi-layered system <gc4.D>

C

C J-PROGRAM, 3-COMPARTMENTS, K-LAYERS

C

GCOMP Source Code



C DEB SUBROUTINE GCOMP(G,X)

C

C PAMELA G. ANDERSON, AUGUST 14, 1995

C SAVE

C Date Description

C -----

- C 8/14/95 PGA Creation of MODFLOW data file written and checked
- C 8/29/95 PGA Conversion to subroutine and addition of MODFLOW call
- C 9/20/95 PGA Added G(2) for second constraint
- C 9/25/95 PGA Added time loop so that data from ALL time steps is used
- C 9/25/95 PGA Changed order of variable to see if has any effect on GRG2

C

C 10/30/95 PGA Revised section reading observation and model data for specific cells

C DO DATA (Note: program reads SPECIFIC cells; change for different data.)<gc3.f>

C 12/6/95 PGA Revised observation data for multi-layered system <gc4.f>

C KEM(K) = X(K\*10)

C I=ROWS, J=COLUMNS, K=LAYERS

C

**GCOMP Source Code**

```

C DECLARATIONS
C
  IMPLICIT REAL*8(A-H,O-Z)
  SAVE
  INTEGER LAYCON(50)
  CHARACTER FMTIN*16, TITLE*10, TRASH*20, HEADR1*80, HEADR2*50
  DIMENSION TRPY(50), DELR(50), DELC(50)
  DIMENSION SF1(50,50), TRANS(50,50), VCONT(50,50)
  DIMENSION DDNMOD(25,25,25)
  DIMENSION G(*), X(*)
  REAL*8 SCM(50), KHM(50), KVM(50)
C
C
C SETTING UP MULTIPLIER ARRAYS
  DO 50 K = 1, 6
    SCM(K) = X(K)
    KHM(K) = X(K+6)
    KVM(K) = X(K+12)
  50
C

```

GCMP Source Code



```

5  ST READ(41,1010)ISS, IBCFCB
   WRITE(42,1010)ISS, IBCFCB
   READ(41,1011)(LAYCON(K), K=1,NL)
   WRITE(42,1011)(LAYCON(K), K=1,NL)
   READ(41,1021)LOCAT,CNSTNT,FMTIN,IPRN, TITLE
   WRITE(42,1021)LOCAT,CNSTNT,FMTIN,IPRN, TITLE
   READ(41,1013)(TRPY(K),K=1,NL)
   WRITE(42,1013)(TRPY(K),K=1,NL)
   READ(41,1021)LOCAT,CNSTNT,FMTIN,IPRN, TITLE
   WRITE(42,1021)LOCAT,CNSTNT,FMTIN,IPRN, TITLE
   READ(41,1013)(DELR(I), I=1,NR)
   WRITE(42,1013)(DELR(I), I=1,NR)
   READ(41,1021)LOCAT,CNSTNT,FMTIN,IPRN, TITLE
   WRITE(42,1021)LOCAT,CNSTNT,FMTIN,IPRN, TITLE
   READ(41,1013)(DELC(J), J=1,NC)
   WRITE(42,1013)(DELC(J), J=1,NC)

```

C-----

C STARTING LOOP FOR EACH LAYER

C DO 20 K = 1, NL PERMEABILITY FOR EACH LAYER

C

C WRITING STORAGE COEFFICIENT FOR EACH LAYER

C

READ(41,1017)CCARD

WRITE(42,1014)SCM(K),K

DO 22 I = 1, NR

READ(41,1013)(SF1(I,J),J=1,NC)

22 WRITE(42,1013)(SF1(I,J),J=1,NC)

C

C WRITING TRANSMISSIVITY FOR EACH LAYER

C

READ(41,1017)CCARD

WRITE(42,1015)KHM(K),K

DO 24 I = 1, NR

READ(41,1013)(TRANS(I,J),J=1,NC)

24 WRITE(42,1013)(TRANS(I,J),J=1,NC)

GCOMP Source Code



```

C
C WRITING VERT. CONDUCTIVITY FOR EACH LAYER
C
      IF(K.EQ.NL)GO TO 20
      READ(41,1017)CCARD
      WRITE(42,1016)KVM(K),K
      DO 26 I = 1, NR
      READ(41,1013)(VCONT(L,J),J=1,NC)
26  WRITE(42,1013)(VCONT(L,J),J=1,NC)
C
C END OF LAYER INFORMATION
20  CONTINUE
C -----
      CLOSE(41)
      CLOSE(42)
C =====
C CALLING MODFLOW TO CALCULATE MODEL DRAWDOWNS
20  CALL MODFLOW

```

GCOMP Source Code

```

C
C
C COMPARING MODEL TO OBSERVED DRAWDOWNS
C
C
C OPEN(UNIT=43,FILE='FOR076.DAT',STATUS='UNKNOWN')
C OPEN(UNIT=45,FILE='OBSERV2.DAT',STATUS='UNKNOWN')
C OPEN(UNIT=46,FILE='OBSERV4.DAT',STATUS='UNKNOWN')
C REWIND(43)
C REWIND(45)
C REWIND(46)
C
C READING DRAWDOWN DATA
C
C
C SDS = 0.0
C G(2) = 0
C
C STARTING TIME LOOP
C
C DO 70 T = 1, 20
C DO 30 K = 1, NL
C READ(43,*)TRASH
C READ(43,*)((DDNMOD(K,I,J), J = 1,NC), I = 1,NR)
C
C 30 CONTINUE

```

**GCOMP Source Code**



```

1017 READ(45,*)TS, DDNOB1
1018 READ(46,*)TS, DDNOB2
C CALCULATING SUM OF DIFFERENCES, G(K)
1020 SDS = SDS+(DDNMOD(5,2,15)-DDNOB1)**2+(DDNMOD(3,2,15)-DDNOB2)**2
C NEXT TIME STEP
70 CONTINUE
C END OF TIME LOOP
CLOSE(43)
CLOSE(45)
CLOSE(46)
C *****
1010 FORMAT(2I10)
1011 FORMAT(40I2)
1012 FORMAT(I10,F10.2," (",A16,2X,I10,2X,A20)
1013 FORMAT(10G10.3)
1014 FORMAT(8X,"11",G10.3,2X,"(", "10G10.3" ,")",17X,"0 SF1-",I2)
1015 FORMAT(8X,"11",G10.3,2X,"(", "10G10.3" ,")",17X,"0 TRANS-",I2)
1016 FORMAT(8X,"11",G10.3,2X,"(", "10G10.3" ,")",17X,"0 VCONT-",I2)

```

GCOMP Source Code

```

17 1
NAME Oxid-2a Multi-Layer Model
ROWS (Function Boundaries)
G 1 80
END
BOUNDS (Variable Boundary)
G 1 1.00E-04
G 2 1.00E-04
G 3 1.00E-04
G 4 1.00E-04
G 5 1.00E-04
G 6 1.00E-04
G 7 1.00E-04
G 8 1.00E-04
G 9 1.00E-04
G 10 1.00E-04
G 11 1.00E-04
G 12 1.00E-04
G 13 1.00E-04
G 14 1.00E-04
G 15 1.00E-04
G 16 1.00E-04
G 17 1.00E-04
END
VARIABLES
SD1
SD2
1017 FORMAT(A20)
1018 FORMAT(4I10)
1019 FORMAT(20A4)
1020 FORMAT(12A4)
1021 FORMAT(I10,F10.0,A20,I10,A20)
1022 FORMAT(9G12.4)
C *****
C PRINTING TO DATA TO DEBUG PROGRAM
G(1) = 100.0*SDS
DO 60 K = 1, 18
60 G(2) = G(2) + X(K)
C
RETURN
END

```

**GCOMP Source Code**



```

17 M1
NAME Oxnard-2a: Multi-Layer Model
ROWS (Function Boundaries)
O 1 0.0
END
BOUNDS (Variable Boundaries)
G 1 1.00E-04
G 2 1.00E-04
G 3 1.00E-04
G 4 1.00E-04
G 5 1.00E-04
G 6 1.00E-04
G 7 1.00E-04
G 8 1.00E-04
G 9 1.00E-04
G 10 1.00E-04
G 11 1.00E-04
G 12 1.00E-04
G 13 1.00E-04
G 14 1.00E-04
G 15 1.00E-04
G 16 1.00E-04
G 17 1.00E-04
END
VARIABLES (Names)
SF1 1
SF2 2
SF3 3
SF4 4
SF5 5
SF6 6

```

**GCOMP Sample Input File**

KHM1 7  
KHM2 8  
KHM3 9  
KHM4 10  
KHM5 11  
KVH6 12  
KVM1 13  
KVM2 14  
KVM3 15  
KVM4 16  
KVM5 17

END

INITIAL

TOGETHER (8E10.4)

1.000	1.000	1.000	1.000	1.000	1.000	1.000	1.000
1.000	1.000	1.000	1.000	1.000	1.000	1.000	1.000
1.000							

PRINT

IPR 4

END

EPS (Tolerance Control)

EPN 1.0E-06

EPI 1.0E-01

EPT 1.0E-16

END

METHOD Selection

FDI

END

GO

STOP

**GCOMP Sample Input File**